

COMPUTATIONAL PROCESS DESIGN, OPTIMIZATION AND GROWTH OF
ZINC OXIDE NANOSTRUCTURES ON GRAPHENE BY ULTRASONIC
SPRAY PYROLYSIS

AMGAD AHMED ALI IBRAHIM

A thesis submitted in fulfilment of the
requirements for the award of degree of
Doctor of Philosophy

Malaysia-Japan International Institute of Technology
Universiti Teknologi Malaysia

MAY 2016

DEDICATION

To the Soul of my uncle,
To my beloved mother and father,
To Safy, Dalia and Xiyan,
To my blessed country: Egypt.

ACKNOWLEDGEMENT

During preparing this thesis, I was in contact with many people, researchers, academicians, and practitioners. They have contributed towards my understanding and thoughts. In particular, I wish to express my sincere appreciation to my main thesis supervisor, associate Professor Dr. Abdul Manaf Hashim, for encouragement, guidance, and care.

I am also indebted to Malaysia-Japan International Institute of Technology (MJIT) for funding my study. Also to Universiti Teknologi Malaysia (UTM) for providing all the facilities required to complete the research. Librarians at UTM also deserve special thanks for their assistance in supplying the relevant literatures.

My fellow postgraduate students should also be recognised for their support especially Mohamad Sarwan, Nur Suhaili Abdul Aziz Nurul Fariha Ahmad, Tahsin Morshed and Ferdawaty Rashidy Wong. My sincere appreciation also extends to all my colleagues and others who have provided assistance at various occasions. Their views and tips are useful indeed. And among them all I'm so grateful to my dear friends Shawqi Al-Rashidy and Mojtaba Alizadeh. Unfortunately, it is not possible to list all of them in this limited space. I am grateful to all my family members.

ABSTRACT

Computational process design, optimization, growth, characterization and computational analysis of zinc oxide (ZnO) nanostructures grown on graphene using zinc acetylacetonate ($\text{Zn}(\text{acac})_2$) in the presence of hydrogen by ultrasonic spray pyrolysis were performed systematically. The dissociation of Zn ions from vapour-phase $\text{Zn}(\text{acac})_2$ and its adsorption onto graphene oxide were studied using quantum mechanics approach involving the use of Density Functional Theory (DFT). The reaction energies were calculated, and the proposed reaction mechanism was well supported by a simulation of infrared properties. Next, Response Surface Methodology (RSM) was used to model and optimize the pyrolysis parameters by evaluating the nanostructure density, size and shape factor. The evolution of ZnO structures was well explained confirming that RSM is a reliable tool for the modelling and optimization of the pyrolysis parameters and prediction of nanostructure sizes and shapes. Finally, a computational analysis of the measured optical and charge transport properties of the grown nanostructures, i.e. Nanosphere Clusters (NSCs), Nanorods (NRs) and Nanowires (NWs) were developed. The calculated absorbance spectra based on the time-dependent DFT showed very close similarity with the measured behaviours. The atomic models and energy level diagrams were developed and discussed to explain the structural defects and band gap. As a conclusion it was found that the induced stress in the ZnO NSCs is the cause of gap narrowing between the energy levels. ZnO NWs and NRs showed homogeneous distribution of the Lowest Unoccupied Molecular Orbitals (LUMO) and Highest Occupied Molecular Orbitals (HOMO) orbitals all over the entire heterostructure which results to the reduction of the band gap. The calculated band gaps are confirmed to be in a good agreement with the experimental results. The electrical models and electrostatic potential maps were able to calculate the electron life time and to explain the mobility and diffusion behaviours of the grown nanostructures, respectively.

ABSTRAK

Proses reka bentuk secara pengkomputeran, pengoptimuman, pertumbuhan, pencirian dan analisis secara pengkomputeran telah dijalankan secara sistematik bagi pertumbuhan struktur nano zink oksida (ZnO) pada grafin menggunakan zink asetilasetonat ($\text{Zn}(\text{acac})_2$) dengan kehadiran hidrogen oleh teknik semburan pirolisis ultrasonik. Pemisahan ion Zn dari fasa wap $\text{Zn}(\text{acac})_2$ dan penjerapannya pada grafin oksida dikaji menggunakan pendekatan mekanik kuantum melibatkan penggunaan Teori Fungsi Ketumpatan (DFT). Tenaga tindakbalas telah dikira dan mekanisma tindakbalas yang dicadangkan telah disokong baik oleh simulasi sifat-sifat inframerah. Seterusnya, Kaedah Tindakbalas Permukaan (RSM) digunakan untuk memodelkan dan mengoptimumkan parameter pirolisis dengan menilai ketumpatan, saiz dan faktor bentuk nanostruktur. Evolusi struktur ZnO telah diterangkan sebaiknya mengesahkan bahawa RSM adalah alat yang dipercayai untuk pemodelan dan pengoptimuman parameter pirolisis dan anggaran saiz dan bentuk nanostruktur. Akhirnya, analisis pengkomputeran bagi sifat optik dan pengangkutan zarah bercas yang dikira bagi pertumbuhan nanostruktur seperti Kluster Nanosfera (NSCs), Nanorod (NRs) dan Nanowayar (NWs) telah dibangunkan. Spektra penyerapan yang dikira berdasarkan pada penggantungan masa DFT menunjukkan persamaan yang sangat dekat dengan perilaku yang dikira. Model atom dan gambar rajah aras tenaga telah dibangunkan dan dibincangkan untuk menerangkan kecacatan struktur dan jurang jalur. Sebagai konklusi didapati bahawa, tekanan teraruh di dalam NSCs ZnO adalah disebabkan jurang yang semakin sempit antara aras tenaga. NWs dan NRs ZnO menunjukkan pengedaran homogen bagi Orbital Terendah tidak Dihuni Molekul (LUMO) dan Orbital Tertinggi Dihuni Molekul (HOMO) pada seluruh heterostruktur yang mengakibatkan pengurangan pada jurang jalur. Jurang jalur yang dikira adalah disahkan berada dalam persetujuan yang baik dengan keputusan eksperimen. Model elektrik dan peta potensi elektrostatik masing-masing boleh dibangunkan untuk mengira jangka hayat elektron dan untuk menerangkan pergerakan dan perilaku penyebaran bagi pertumbuhan nanostruktur.

TABLE OF CONTENTS

CHAPTER	TITLE	PAGE
	DECLARATION	ii
	DEDICATION	iii
	ACKNOWLEDGEMENT	iv
	ABSTRACT	v
	ABSTRAK	vi
	TABLE OF CONTENTS	vii
	LIST OF TABLES	xi
	LIST OF FIGURES	xii
	LIST OF ABBREVIATIONS	xvii
	LIST OF SYMBOLS	xix
	LIST OF APPENDICES	xxi
1	INTRODUCTION	1
	1.1 Research Background and Motivation	1
	1.2 Problem Statement	4
	1.3 Objectives of the Study	6
	1.4 Scope of the Study	7
	1.5 Contribution of the Present Work	9
	1.6 Overview of Thesis Organization	9
2	SYNTHESIS OF ZnO/GRAPHENE HYBRID STRUCTURES AND ITS POTENTIAL APPLICATIONS	12
	2.1 ZnO Properties	12
	2.1.1 Properties and Device Applications	13

2.2	Properties of Graphene	15
2.3	Overview of ZnO Structures and its Synthesis Methods	19
2.3.1	ZnO Thin Films	19
2.3.2	ZnO Nanoparticles	23
2.3.3	ZnO Nanorods	25
2.3.4	ZnO Nanowires	27
2.4	Ultrasonic Spray Pyrolysis	32
2.4.1	Asynchronous Pulse Ultrasonic Spray Pyrolysis	32
2.4.2	Electrostatic Assisted Ultrasonic Spray Pyrolysis	33
2.4.3	Infrared Ultrasonic Spray Pyrolysis	34
2.4.4	Flame-Assisted Ultrasonic Spray Pyrolysis	36
2.5	Overview of Quantum Chemistry Calculation	37
2.5.1	Density Functional Theory Background	37
2.5.2	Local Density Approximation	39
2.5.3	Exchange Functionals of Density and Density Gradient	40
2.5.4	B3LYP Correlation Functional	41
2.5.5	Use of DFT to Investigate Reaction Mechanisms of Deposition of Metal Oxides	43
3	COMPUTATIONAL AND EXPERIMENTAL BASED DESIGN OF ULTRASONIC ASSISTED SPRAY PYROLYSIS PROCESS	45
3.1	Introduction	45
3.2	Quantum Chemistry Computation	46
3.2.1	Computational Details	48
3.2.2	Validation of the DFT Calculations	51
3.3	Process Design and Statistical Modelling	51
3.3.1	Materials	51
3.3.2	Equipments	52
3.3.3	Ultrasonic Assisted Pyrolysis System	53
3.3.3.1	Design of the Ultrasonic Pyrolysis Reactor	53
3.3.4	Response Surface Methodology RSM	57

4	DENSITY FUNCTIONAL THEORY STUDY OF CHEMICAL DEPOSITION OF ZINC OXIDE ON GRAPHENE FROM GAS-PHASE	62
	4.1 Introduction	62
	4.2 Optimized Geometries	63
	4.3 Reaction Mechanism	66
	4.4 Reaction by-Products	69
	4.5 Validation of Computational Work	74
	4.6 Conclusions	78
5	STATISTICAL ANALYSIS, MORPHOLOGICAL STUDY AND REACTION KINETICS OF THE GROWTH OF ZINC OXIDE NANOSTRUCTURES ON GRAPHENE USING ULTRASONIC SPRAY PYROLYSIS	79
	5.1 Fitting of the Response	79
	5.2 Results and Discussion	81
	5.2.1 Morphological Properties	81
	5.2.2 Structural Properties	83
	5.2.3 Statistical Analysis of the Response	84
	5.2.3.1 Nanowire Density	87
	5.2.3.2 Growth Rate and Kinetics	90
	5.2.3.3 Nanowire Shape Factor	93
	5.2.3.4 Nanowire Size	99
	5.3 Effect of Carrier Gas Flow	102
	5.4 Conclusion	104
6	OPTICAL AND TRANSPORT PROPERTIES OF SYNTHESIZED HYBRID -STRUCTURES	105
	6.1 Introduction	105
	6.2 Optical Properties	106
	6.2.1 Optical Absorption	106
	6.2.2 Time Dependant DFT Band Gap Calculations	109
	6.2.3 Photoluminescence	115

6.3	Electronic Properties	116
6.3.1	Electrochemical Impedance Spectroscopy	116
6.4	Shape Factor Effect	124
6.5	Conclusion	125
7	CONCLUSION AND FUTURE WORK	127
7.1	Conclusions	127
7.2	Directions of Future Work	130
	REFERENCES	133
	Appendix A	156-157

LIST OF TABLES

TABLE NO.	TITLE	PAGE
2.1	Physical parameters of graphene	18
2.2	Comparison of methods reported for growing ZnO nanostructures on graphene from liquid and gas phase	30
2.3	Results of the G2/97 assessment for various local density approximation approaches	40
3.1	Selected levels for process parameters used during experiments	59
3.2	Typical RSM $L_{16}(4^4)$ array of the combinations of parameters for the experimental runs	61
4.1	Computed atomic charges calculated for the keto and enol tautomers of acetylacetonate molecule	72
4.2	Computed bond orders and bond lengths for the keto and enol tautomers of the acetylacetonate molecule	73
4.3	Results of the IR simulation compared to published experimental results	76
5.1	RSM $L_{16}(4^4)$ array of the combinations of parameters for the experimental runs	80
5.2	Summary of ANOVA results for the fitted responses	85
5.3	Values of the constants used in equation 5.1	87
5.4	Values of the constants used in equation 5.8	94
5.5	Values of the constants used in equation 5.9	99
7.1	Summary of photovoltaic parameters of various ZnO/graphene hybrid structures	132

LIST OF FIGURES

FIGURE NO.	TITLE	PAGE
1.1	Evolution of Si-based nanoelectronics	2
1.2	Flow chart summarizing the scope of work	8
2.1	Forms of sp ² -bonded carbon of fullerene, single-walled carbon nanotubes, graphene and graphite	16
2.2	Honeycomb lattice, the vector δ_1 , δ_2 , and δ_3 connect nearest neighbor carbon atoms, separated by distance $a = 0.142\text{nm}$. The vectors a_1 and a_2 are basis vectors of the triangular Bravais lattice	17
2.3	Schematic of the graphene structure with (a) zigzag edge and (b) armchair edge	18
2.4	Schematic illustrations for the AP-UASP system. 1 substrate, 2 heating furnace, 3 atomizer, 4 carrier gas, 5 precursor solution, 6 diaphragm and 7 ultrasonic nebulizer	33
2.5	Schematic illustration of the electrostatic assisted USAP system	34
2.6	Schematic of LASP: (1) laser through optical fiber, (2) oxygen inlet, (3) T-shaped quartz tube, (4) substrate, (5) heater, (6) raster stage, (7) temperature controller, (8) ultrasonic atomizer and (9) carrier gas inlet. Inset (a) horizontal and (b) vertical scan [150]	35
2.7	Schematic representation of the FAUSP system [159]	36
3.1	Conceptual frame work of the methodology used in this research	46
3.2	Possible routes of deposition of ZnO from gas phase	47

3.3	Schematic of (a) SL graphene and (b) SEM images of SL graphene where, the darker area shows the thicker graphene layer	52
3.4	Homemade UASP system with modified cover head	54
3.5	Flow directions of N ₂ gas through the reactor cover	55
3.6	Calculated heat distribution at 35mbar vacuum, 355 substrate temperature and 250 SCCM gas flow rate	56
3.7	Schematic representation of parameters combination network for experimental runs	60
4.1	Structures and geometries of transition states, intermediates and products in the dissociation reaction (route (A))	63
4.2	Structures and geometries of transition states, intermediates and products in the dissociation reaction (Route (B))	65
4.3	Potential energy profile showing relative energies for dissociation reaction calculated with B3LYP/6-311+G(d,p) level of theory for the ALD	67
4.4	Potential energy profile showing relative energies for dissociation reaction calculated with B3LYP/6-311+G(d,p) level of theory for the alcohol assisted pyrolysis	69
4.5	Merged electrostatic potential map (isosurface) and spin density map (isocontours) for acac enol tautomer (a) and Keto tautomer (b)	71
4.6	Results of IR simulation for the Zn-H adsorption onto graphene oxide matrix calculated using DFT and corresponding optimized structure for various Zn ²⁺ adsorption reaction steps	75
4.7	Energy profile calculations for the adsorption of ZnO onto different positions on the graphene matrix	77
5.1	Top view FESEM images that resulted from the (a) R4, (b) R9, (c) R7 and (d) R16 experimental runs	82
5.2	XRD patterns of the ZnO nanowires grown at experimental combination runs of R4, R7, R9 and R16	84

5.3	3D plots that depict the interactions between the process parameters and their impact on the nanowire density, size and shape factor	86
5.4	3D Relationship between nanowire density and (a) precursor flow rate, (b) precursor molarity, (c) injection time and (d) substrate temperature based on single factorial analysis	88
5.5	The relation between the growth rate and substrate temperature	92
5.6	Arrhenius plot represents the relation between the logarithm of kinetic constants (ordinate axis) plotted and the inverse temperature (abscissa)	93
5.7	Normal probability plot for nanowire shape factor fitting.	95
5.8	The relationship between the shape factor of the nanowires and the molarity of precursor at constant injection time ($t = 15.25$ min), constant temperature ($T = 134$ °C) and constant precursor flow rate ($Q = 8$ ml/min)	96
5.9	Phase transformation diagrams depicting the relationship between the precursor molarity and the substrate temperature, structure density and structure shape	97
5.10	TEM images of nanowires grown at a substrate temperature of 240 °C, 0.2 M precursor molarity of 0.2 M, flow rate of 0.05 ml/min and injection time of 10 min	98
5.11	Relationships between the calculated growth rate and the nanowire size and injection time	101
5.12	The relationship between the droplet size of the atomized precursor and the size of the resulting nanowires	102
5.13	Schematic illustration of the trapped spray droplets at the carrier gas turbulent eddies at St less than 1	103
6.1	The optical absorption spectra of various ZnO nanostructures/graphene samples	107
6.2	The $(\alpha h\nu)^2$ versus $(h\nu)$ for (a) ZnO-NRs, (b) ZnO-NRs and (c) ZnO-NSC based heterostructures	109

6.3	Comparison between the calculated and measured UV-Vis spectra and the corresponding atomic model for (a) ZnO-NRs, (b) ZnO-NWs, and (C) ZnO-NSC based heterostructures	110
6.4	The FTIR spectra of various ZnO/graphene hybrid structures	111
6.5	Energy levels diagram for the ZnO-NSC nanostructure at excited state	113
6.6	Energy levels diagram for the ZnO-NWs at excited state.	114
6.7	Emission spectra of ZnO /graphene hybrid structures (a), Schematic representation of the intersystem crossing(band-bonding effect) (b)	116
6.8	3 electrode setup used during the electrochemical spectroscopy (EIS) measurements.	117
6.9	Results of EIS measurements for the ZnO-NRs /graphene. (a) Nyquist plot, (b) Bode plot and (c) equivalent fitted circuit	118
6.10	Schematic representation for sample-electrolyte interface based on the stern model	119
6.11	Schematic representation for sample-electrolyte interface based on the stern model for the ZnO-NRs/graphene hybrid structure	120
6.12	Results of EIS measurements for the ZnO-NWs/graphene. (a) Nyquist plot, (b) Bode plot and (c) equivalent fitted circuit	121
6.13	Electrostatic map for the ZnO-NWs /graphene hybrid structure. The blue areas represent the channels with highest electrostatic potential, whereas the red areas are representing the forbidden areas for negatively charged particles	122
6.14	Results of EIS measurements for the NSC ZnO /graphene. (a) Equivalent fitted circuit, (b) Nyquist plot and (c) Bode plot	123

6.15	Electrostatic map for the ZnO-NSC/graphene hybrid structure. The blue areas represent the channels with highest electrostatic potential, whereas the red areas are representing the forbidden areas for negatively charged particles	124
6.16	Nyquist plot and the UV/Visible spectra respectively for nanorods with various shape factors.	125
7.1	Current density versus voltage for the ZnO/graphene hybrid structures under the light of 450 W xenon lamp	131

LIST OF ABBREVIATIONS

1D	-	One dimensional
2D	-	Two dimensional
Au	-	Gold
CMOS	-	Complementary metal-oxide semiconductor
CNT	-	Carbon nanotube
Cu	-	Copper
CVD	-	Chemical vapour deposition
DI	-	Deionized
DLE	-	Deep level emission
EDX	-	Energy dispersive X-ray
FESEM	-	Field emission scanning electron microscope
FWHM	-	Full width half maximum
GaAs	-	Gallium arsenide
GaN	-	Gallium nitride
Ge	-	Germanium
GOI	-	Ge-on-insulator
He-Cd	-	Helium-cadmium
HMTA	-	Hexamethylenetetramine
i-SOC	-	Intelligent technology system-on-chip
LED	-	Light emitting diode
ML	-	Multilayer
MOVPE	-	Metal organic vapour phase epitaxy
NBE	-	Near band edge
O ₂	-	Oxygen
OH ⁻	-	Hydroxide
PL	-	Photoluminescence
Pt	-	Platinum

RT	-	Room temperature
Si	-	Silicon
SiC	-	Silicon carbide
Si-LSIs	-	Silicon-large scale integrated circuits
SiO ₂	-	Silicon dioxide
SL	-	Single layer
ST	-	Set temperature
TEM	-	Transmission electron microscope
ULSIs	-	Ultra large scale integrated circuits
UV	-	Ultraviolet
XRD	-	X-ray diffraction
Zn	-	Zinc
Zn(NO ₃) ₂ ·6H ₂ O	-	Zinc nitrate hydroxide
ZnO	-	Zinc oxide

LIST OF SYMBOLS

a	-	Basic vector of the triangular Bravais lattice
\AA	-	Angstroms, $1\text{\AA} = 1 \times 10^{-10} \text{ m}$
b	-	Regression coefficient
$^{\circ}\text{C}$	-	Degree Celsius
cm	-	Centimetre
cm^2/Vs	-	Square centimeter per volt second
d_p	-	atomized spray droplet size
e	-	Statistical fitting error
eV	-	Electron volt
$E_{xc}(\rho)$	-	Exchange-correlation energy functional
GHz	-	Gigahertz
I_N	-	Power surface intensity of sonicator
M	-	Molarity of precursor solution
$mAh g^{-1}$	-	Mili amper hour per gram
nm	-	Nanometre
m^2/g	-	Square metre per gram
mA/cm^2	-	Miliampere per square centimetre
meV	-	Mili-electron volt
ms^{-1}	-	Metre per second
mW	-	Miliwatt
n	-	An integer 1, 2, 3 (usually equal to 1)
N	-	Corresponding number of carbon chain
nm	-	Nanometre
Oh	-	Ohnesorge number
Q	-	Liquid precursor flow rate
r	-	Nanostructure size (radius)
r_i	-	Distance between charged particle and atom center

S_t	-	Stokes number
t	-	Injection time
T	-	Substrate temperature
U	-	Carrier gas flow rate
W_{ac}	-	Width for armchair
W/mK	-	Watt per metre per Kelvin
wt%	-	Weight percent ratio
W_{zz}	-	Width for zigzag
χ	-	Independent parameters
y_i	-	Taylor's function response
Zn^{2+}	-	Zinc dication
α	-	Significance level
ψ_I	-	Slater tensor of orthonormal orbitals
$\psi_{i\sigma}$	-	Occupied spin orbitals
δ	-	Lattice vector
ε_p	-	Electrostatic potential
φ	-	Nanostructure shape factor
φ_i	-	Basis set function
λ	-	Wavelength in angstroms
μm	-	Micrometre
v_{ext}	-	External nuclear potential
θ	-	Diffraction angle in degrees
ρ	-	Droplet density
ρ^{spin}	-	Spin density
ρ^α	-	Electron density formed by electrons of α spin
ρ^β	-	Electron density formed by electrons of β spin
σ	-	Surface tension
ζ	-	Nanowire density

LIST OF APPENDICES

APPENDIX	TITLE	PAGE
A	List of Publications	156

CHAPTER 1

INTRODUCTION

1.1 Research Background and Motivation

According to the Moore's law, the capability of silicon-large scale integrated circuits (Si-LSIs) was improved over the last three decades by increasing the population of transistors on the substrate [1, 2]. The most recent processors contain over a billion transistors. A remarkable enhancement for the efficiency of the ultra large scale integrated circuits (ULSIs) was achieved by following a scaling-up routine for the silicon (Si) transistor. However, further enhancement of the efficiency of the LSIs turn out to be more complicated as a result of the transistors contraction (which is attributed to physical limitations) [3].

Advanced heterogeneous integration on Si platform has recently attracted great attention towards the understanding of a so-called "More than Moore" technology. This approach is mainly devoted to the growth of high quality elements (i.e. germanium (Ge) [4, 5]) and semiconductors based compounds such as gallium arsenide (GaAs) [6-8], gallium nitride (GaN) [9-12] and silicon carbide (SiC) [13], as well as metal oxides (i.e. zinc oxide (ZnO) [14, 15] and carbon based materials such as graphene [13, 16, 17] and carbon nanotube (CNT) [18-20] on Si platform. In fact, the cointegration of such materials led to the present ULSIs with ultra-high speed complementary metal-oxide semiconductor (CMOS) transistors [20, 21] in addition to various kinds of functional devices as optical devices [22-24], photodetectors [25-27], sensors and solar batteries [28]. Thus, such Si based intelligent system-on-chip (i-SoC) is considered to be promising.

The Si based system-on-chip technology is considered as a new generation technology. This is ascribed to its ability to present more capable and practical routes of development of electronic devices. An insulator that electronically isolates the functional materials from the Si substrate found to be essential for producing electronic devices. In accordance to this context, various researches reported the growth of high quality Ge-on-insulator (GOI) [29, 30], graphene-on-insulator [31-33], GaAs-on-insulator [8, 33-35], SiC-on-insulator [36-38] and ZnO-on-insulator structures [39]. Figure 1.1 illustrates the evolution of the Si based nano-electronics device. The integration of devices on Si platform in the way shown in figure was reported to improve the functionality, the quality and the efficiency of the device system.

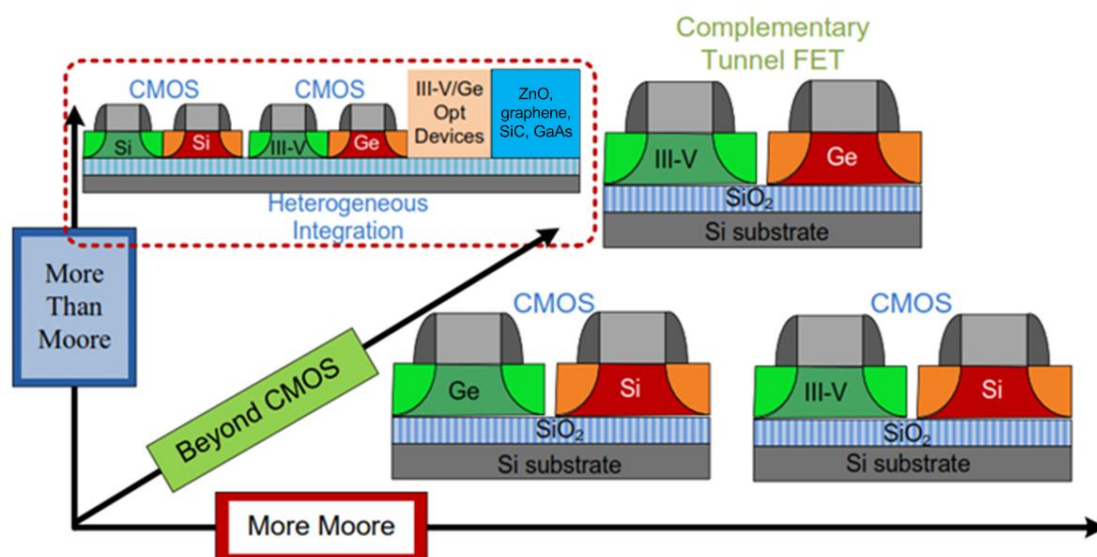


Figure 1.1 Evolution of Si-based nanoelectronics [40, 41]

Modern electronic devices are much depending on transparent conductive thin films (TCFs). Many applications are currently using TCFs such as field emission displays, sensors, thin film transistors solar cells, touch panels, electrostatic dissipation, and transparent electrodes for optoelectronic devices [42]. In fact, the development of alternative materials for such applications is taking place. For instance, the optically transparent and electrically conductive material Indium-Tin-Oxide (ITO) exhibits a sheet resistance and light transmittance that is meeting the standard requirement. However, ITO is not maintaining sufficient flexure stiffness.

Researchers have succeeded in preparing TCFs with single-walled carbon nanotubes (SWCNT) [43-45].

Recently, graphene nanosheets (GNS) were discovered, which can be obtained by the reduction of graphene oxide (GO). Two-dimensional (2D) sheet of sp²-hybridized carbons known as graphene has attracted great attention because of its exceptional optical, electrical, chemical and mechanical properties that imposes promising ability for developing new generation of functional nanomaterials for various applications [1-3]. A lot of research on graphene has stimulated the development of high-quality graphene for optoelectronic devices [1]. An ideal monolayer of graphene has an excellent light transmittance and conductivity at room temperature. Such optoelectronic properties suggest graphene as a promising material for flexible transparent conductor [3]. Lately, various methods were reported for growing graphene for large area production. Chemical vapour deposition (CVD) is the most used method for preparing high quality large-area monolayer graphene. Such method can control thickness of deposited layers for possible application as transparent conductors. Generally, GNS are found to be more conductive, flexible and less expensive than ITO or SWCNTs for transparent electrode applications [2].

Concerning the targeted applications, there have been huge exerted efforts to control and modify the properties of graphene through various functionalization routes [46-49]. The combination of various types of materials can lead to development of new generations of materials that have tailored properties suitable for new optoelectronic applications, which is beyond the ability of the individual materials. Thus decorating two-dimensional (2D) graphene with one-dimensional (1D) semiconductor nanostructure phase can result in a three-dimensional (3D) multifunctional conductor. It was reported in different studies the preparation of 1D-2D hybrid architectures (HAs) composed of regular arrays of nanorods such as zinc oxide, silver, platinum, palladium and gold formed on graphene layers. The 1D-2D HAs exhibited outstanding electrical conductivity, optical transparency, and mechanical flexibility, comparable to those of graphene. There are few studies that

compare the effect of the metallic nano-rods material on the property of the multifunctional conductor [46-49].

Nanowires as prolonged nanostructures have privileges over other nanostructures. For instance, their electrical transport properties are much better than those of nanoparticles because of the extended transport surface area of nanowires. Besides, the optical reflectance of the nanorods is less than thin films thus, significantly their absorption of light increases, which is particularly interesting for photovoltaic and photon-induced hydrophilicity applications [50, 51]. Furthermore, much research has been conducted for developing semiconducting material/graphene hybrid structures either by vapour-phase [52-54] or liquid-phase techniques [55-57]. Since the past few decades, ZnO nanostructures have been thoroughly considered in many works for optoelectronic and photovoltaic device applications [58-61]. Recently, it has been reported that ZnO/graphene hybrid nanostructure has excellent potential to be used for transparent flexible electrical and optical devices, including flexible photovoltaics, displays, and light emitters [62-64].

1.2 Problem Statement

Majority of literatures are reporting on ZnO/graphene hybrid structures focus on the discussion of the structural morphologies [48]. Very few researches focused on the optimization of the process parameters [65, 66]. In fact, there is no report on the statistical modelling and subsequent optimization of the growth of ZnO nanowires on graphene using ultrasonic spray pyrolysis (UASP). Most of experimental design in such field is based on single factor design that leads to data waste, excessive precursor consumption and longer growth time in addition to lack of reproducibility upon scaling-up reactions. Thus, the effect of process parameters on the grown structures are not yet clear, for instance, the effect of the process parameters on ZnO density, shape and size of grains is not clearly reported. Furthermore, the ultrasonic assisted spray pyrolysis is mentioned mostly in articles for film deposition, however very scarce articles targeted the process ability for

depositing other ZnO nanostructures. Thus, there is a need to clarify the capability of the process to deposit other categories of ZnO nanostructures such as quantum dot, nanowires and any other possible structures.

In order to suit graphene for optoelectronic devices, research works have been carried out to develop graphene based materials hybrid with semiconducting structures through various processes such as vapour-phase [52-54] or liquid-phase deposition techniques [55-57]. The vapour-phase deposition of ZnO using β -diketonates such as acetylacetonate as the Zn precursor was reported as a promising route to grow ZnO nanostructures [67, 68]. However, most studies on ZnO/graphene hybrid structures have focused on their structural morphologies and electronic properties [69], whereas few have paid attention to the reaction mechanisms of the semiconducting species at reaction sites on the graphene surface [65, 70]. There is no report to date on the reaction mechanisms of the vapour-phase deposited ZnO onto graphene utilizing acetylacetonate as a Zn source. In the current research, the possible reaction mechanisms that take place during the deposition of ZnO on graphene based substrates are investigated.

In this study, the growth of ZnO nanowires onto graphene as insulator using a low-temperature ultrasonic assisted spray pyrolysis technique was done. It is a simple and potentially industrially scalable process due to the abundance and stability of the precursors, and the low maintenance and set-up costs involved in scaling-up the process. Besides, it allows the deposition of homogeneous metal oxide phases, endowed with excellent physical properties for several applications. In addition, this work aimed to investigate the capability of the ultrasonic assisted spray pyrolysis for the deposition of every possible ZnO structure on graphene layer. Statistical modelling was used in correlation to multi-factorial experimental design to investigate the impact of the parameters of the process on the density, size and shape of the grown ZnO.

The injection of zinc acetylacetonate in the presence of either alcohol or hydrogen was studied, which are the main deposition routes using spray pyrolysis as found in literature [71, 72]. Quantum chemistry calculation approach is used to identify the most favoured route from the point of view of reaction kinetics taking in consideration the reduction of deposition temperature. Finally, various characterization techniques such as energy dispersive X-ray spectroscopy (EDX), fourier transform infrared spectroscopy (FTIR), field emission electron microscopy (FESEM) and energy dispersive spectroscopy (EDS) were used to investigate the structures morphology. Photoluminescence (PL) measurements, UV/Visible spectroscopy and electrochemical impedance (EIS) were used in combination with density functional theory calculations (DFT) (in the excited state of matter) to investigate the optoelectronic properties of the synthesized hybrid material.

1.3 Objectives of the Study

The objective of the present study is to prepare and characterize graphene based heterogeneous material hybrid with different ZnO nanostructures (mainly nanowires) for optoelectronic applications using ultrasonic assisted spray pyrolysis from liquid precursors. The objective can be divided into the following sub-objectives:

1. To propose growth mechanism using quantum chemistry calculation approach.
2. To design and construct a homemade ultrasonic assisted spray pyrolysis system.
3. To grow ZnO nanowires onto graphene layer and investigate the capability of the process to grow other ZnO nanostructures on graphene layer.
4. To optimize the deposition parameters and develop a statistical model to predict the growth rates and reaction kinetics using response surface method (RSM).

5. To investigate the optical and charge transport properties of the obtained structures using analytical and materials research aspects.

1.4 Scope of the Study

To achieve the objective of this study, the work was performed in three phases; i) Identify the favoured route for deposition of ZnO nanostructures on graphene layer from point of view of reaction kinetics using quantum chemistry approach, ii) grow ZnO nanowires on graphene layer, iii) Optimize the process of growth of ZnO nanostructures on graphene layer and iv) characterize the obtained samples. Figure 1.2 presents a flow chart summarizing the scope of this study. The details of the scope of the present study cover the following stages:

1. Preparation of deposition mixtures of various precursors-solvents mixing ratios.
2. Deposition of ZnO nanostructures on graphene layers under various reaction conditions.
3. Establishing the effects of deposition conditions on the ZnO growth rates and reaction kinetics.
4. Optimization of the growth reaction parameters using RSM.
5. Determination of various opto-electrical properties of the prepared conductor as well as investigating its morphology.

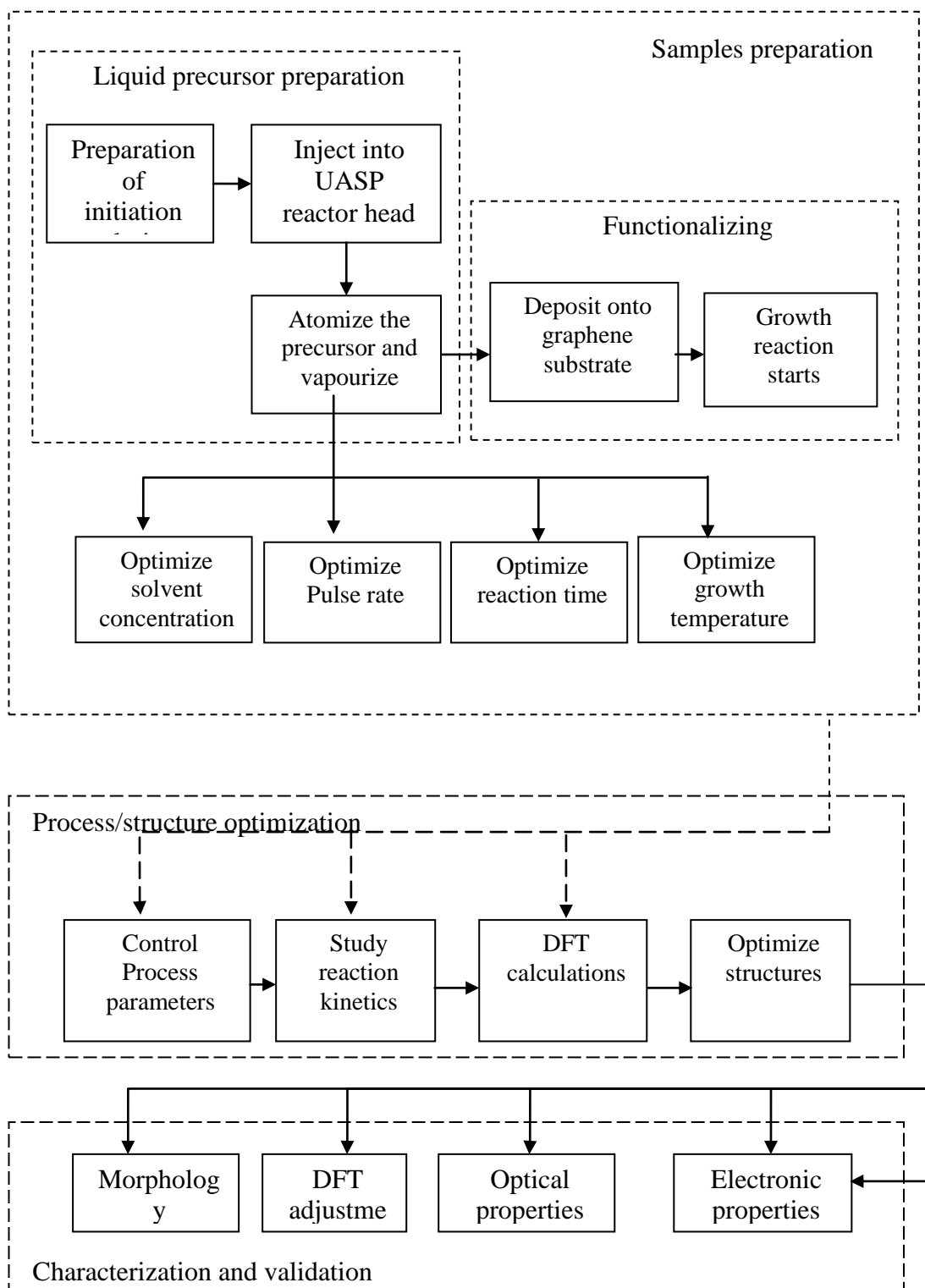


Figure 1.2 Flow chart summarizing the scope of work

1.5 Contribution of the Present Work

The main contribution of the present study can be divided into 3 major parts. The first part comprises of verifying the ability of the UASP process to deposit various ZnO nanostructures on SL graphene at relatively low substrate temperatures (134 – 355 °C) as well as establishing the growth rates and kinetics for all obtained structures using statistical tools. On the other hand, the second part of the contribution is identifying the favoured reaction pathway and the optimized geometries of transitions, intermediates and products by investigating the chemistry of possible pyrolysis routes and its corresponding reaction mechanisms using quantum chemistry approach. Lastly, the last part of the contributions is attributed to the exploration of optical properties of the ZnO/graphene hybrid structures as well as establishing the transport mechanisms of the charged particles through the obtained structures.

1.6 Overview of Thesis Organization

This thesis is structured on 6 chapters. First chapter highlights the overview of the research background and motivation of the past and current work on the growth of ZnO nanostructures on graphene. Besides, the research objectives and scopes are also included. Second chapter includes the overview of the main properties of ZnO and graphene. Furthermore, a brief description about the methods reported for growing ZnO on the graphene is included. Various research works on the impact of the morphology of different ZnO nanostructure on the optoelectronic properties of ZnO/graphene heterogeneous materials are briefly presented in chapter 2. The function of graphene as a buffer layer is also highlighted. Moreover, an overview of the use of ultrasonic assisted spray pyrolysis process to grow ZnO nanostructures on graphene is also included. Finally, the potential applications of ZnO on the graphene regarding the development of optoelectronic devices are also discussed in this chapter.

The third chapter of this thesis contains a brief discussion about the properties of the substrates used in this study. The group of materials, chemicals and equipment used throughout the entire research work are also listed in this chapter. The density functional theory approach in addition to other quantum chemistry calculations is discussed and the possible reaction mechanism of pyrolysis is presented as well. Furthermore, the aspects of multi factorial experimental design were presented, where RSM experimental design approach is followed. Finally, the ultrasonic assisted pyrolysis process is discussed in relation to reactor design and the main process parameters are clarified as well.

The fourth chapter of the thesis presents the results of the DFT study of the dissociation mechanisms of either zinc ions (Zn^{2+}) or ZnO from vapour-phase zinc acetylacetonate, $\text{Zn}(\text{C}_5\text{H}_7\text{O}_2)_2$ and its adsorption onto graphene layer. Moreover, the gas-phase reactions followed during the deposition of zinc oxide on graphene to produce ZnO/graphene composite had been investigated using two different routes. The energies of reactants, transition states and products were calculated and the reaction mechanisms were presented also.

The fifth chapter of this thesis includes a discussion about the experimental design and the results of the RSM modelling. The impact of the process parameters on the nanostructures density, size and shape is thoroughly discussed. The growth rates and reaction kinetics are also presented in this chapter. Furthermore, the structural morphology of ZnO nanostructures is systematically characterized. The involved growth mechanism is studied and described.

The sixth chapter of this thesis includes the discussion about the optoelectronic properties of the grown structures. UV/Visible spectra as well as PL spectra were presented in addition to DFT results to investigate the optical properties of the grown structures. Moreover, EIS results in correlation to quantum chemistry calculations of the electrostatic potential were presented to explain the electronic behaviour of the grown structures. Finally, the seventh chapter of this thesis includes

conclusive remarks in addition to the contributions of present work and discussion about future research work and possible study extensions.

REFERENCES

1. Iwai, H. (2011). Materials and Structures for Future Nano CMOS. *Proceedings of the Nanotechnology Materials and Devices Conference*. 23-27 October. Jeju, Korea, 318-315.
2. Yutaka Urino, N. H., Kenji Mizutani, Tatsuya Usuki, Junichi Fujikata,, Koji Yamada, T. H., Takahiro Nakamura, and Yasuhiko Arakawa. (2015). First Demonstration of A thermal Silicon Optical Interposers With Quantum Dot Lasers Operating up to 125 °C. *J. Lightwave Tech.* 33(16), 1223-1229.
3. Astuti, B., Tanikawa, M., Rahman, S., Yasui, K. and Hashim, A. (2012). Graphene as a Buffer Layer for Silicon Carbide-on-Insulator Structures. *Materials*. 5(12), 2270-2279.
4. Kamata, Y., Ikeda, K., Kamimuta, Y. and Tezuka, T. (2010). High-k/Ge p- and n-MISFETs with Strontium Germanide Interlayer for EOT Scalable CMIS Application. *Proceedings of the VLSI Technology (VLSIT)*. 15-17 June. Tokyo, Japan, 189-190.
5. Berbezier, I., Aqua, J. N., Aouassa, M., Favre, L., Escoubas, S., Gouyé, A. and Ronda, A. (2014). Accommodation of SiGe Strain on A Universally Compliant Porous Silicon Substrate. *Phy. Rev. B*. 90(3), 353-359.
6. Sheng, X., Robert, C., Wang, S., Pakeltis, G., Corbett, B. and Rogers, J. A. (2015). Transfer Printing of Fully Formed Thin-film Microscale GaAs Lasers on Silicon with A Thermally Conductive Interface Material. *Las. Photo.s Rev.* 9(4), L17-L22.
7. Kumari, S., Gustavsson, J. S., Wang, R., Haglund, E. P., Westbergh, P., Sanchez, D. and Baets, R. (2015). Integration of GaAs-based VCSEL Array on SiN Platform with HCG Reflectors for WDM Applications. *Proceedinigs of SPIE*. 25-28 February. Istanbul, Turkey, 93720U-93720U-7

8. He, Y., Wang, J., Hu, H., Wang, Q., Huang, Y. and Ren, X. (2015). Coalescence of GaAs on (001) Si Nano-trenches Based on Three-stage Epitaxial Lateral Overgrowth. *App. Phy. Lett.* 106(20), 202-205.
9. Liu, Q., Shi, Z., Zhu, G., Wang, W., Wang, Z. and Wang, Y. (2015). Freestanding GaN Grating Couplers at Visible Wavelengths. *J. Optics.* 17(4), 645-651.
10. Köck, H., Chapin, C. A., Ostermaier, C., Häberlen, O. and Senesky, D. G. (2014). Emerging GaN-based HEMTs for Mechanical Sensing Within Harsh Environments. *Proceedings of SPIE.* 25-28 February. Istanbul, Turkey, 93731U-93731U-5
11. Wośko, M., Paszkiewicz, B., Szymański, T. and Paszkiewicz, R. (2015). Optimization of AlGaN/GaN/Si(111) Buffer Growth Conditions for Nitride Based HEMTs on Silicon Substrates. *J. Cryst. Growth.* 414, 248-253.
12. Lee, H. S., Li, Z., Sun, M., Ryu, K. and Palacios, T. (2013). (Invited) Hybrid Wafer bonding and Heterogeneous Integration of GaN HEMTs and Si (100) MOSFETs. *ECS Transactions.* 50(9), 1055-1061.
13. Dong, R., Guo, Z., Palmer, J., Hu, Y., Ruan, M., Hankinson, J. and Heer, W. A. d. (2014). Wafer Bonding Solution to Epitaxial Graphene–Silicon Integration. *Journal of Physics D: App. Phys.* 47(9), 394-401.
14. Molaei, R., Bayati, M. R., Alipour, H. M., Estrich, N. A. and Narayan, J. (2014). Nanosecond Laser Switching of Surface Wettability and Epitaxial Integration of c-axis ZnO Thin Films with Si(111) Substrates. *Journal of Physics: Cond. Matter.* 26(1), 15-24.
15. García-Gancedo, L., Milne, W. I., Luo, J. K. and Flewitt, A. J. (2013). Sensors Based on SAW and FBAR Technologies. *Proceedings of SPIE.* 25-28 February. Istanbul, Turkey, 879308-879308-7
16. Norris, K. J., Garrett, M., Coleman, E., Tompa, G. S., Zhang, J. and Kobayashi, N. P. (2014). Graphene Mediated Growth of Polycrystalline Indium Phosphide Nanowires and Monocrystalline-core, Polycrystalline-shell Silicon Nanowires on Copper. *J. Cryst. Growth.* 406, 41-47.
17. Oakes, L., Westover, A., Mares, J. W., Chatterjee, S., Erwin, W. R., Bardhan, R. and Pint, C. L. (2013). Surface Engineered Porous Silicon for Stable, High Performance Electrochemical Supercapacitors. *Sci. Rep.* 3, 31-37.

18. Zhao, D., Yang, Z., Wei, H. and Zhang, Y. (2011) Controlled Growth and Supercapacitive Behaviors of CVD Carbon Nanotube Arrays. *Mat. Sci. Forum.* 688, 11-18.
19. An, J., Zhan, Z., Hari Krishna, S. V. and Zheng, L. (2014). Growth Condition Mediated Catalyst Effects on the Density and Length of Horizontally Aligned Single-walled Carbon Nanotube Arrays. *Chem. Eng J.* 237, 16-22.
20. Wei, S., Kang, W. P., Davidson, J. L. and Huang, J. H. (2008). Supercapacitive Behavior of CVD Carbon Nanotubes Grown on Ti Coated Si Wafer. *Diam. Rel. Mat.* 17(4-5), 906-911.
21. Abutaleb, M. M. (2015). A New Static Differential Design Style for Hybrid SET-CMOS Logic Circuits. *J. Comp. Elec.* 14(1), 329-340.
22. Kimerling, L. C. and Michel, J. (2011). Monolithic Microphotonic Integration on the Silicon Platform. *ECS Transactions.* 41(7), 3-13.
23. Zaima, S., Nakatsuka, O., Shimura, Y., Adachi, M., Nakamura, M., Takeuchi, S., Loo, R. (2011). (Invited) GeSn Technology: Impact of Sn on Ge CMOS Applications. *ECS Transactions.* 41(7), 231-238.
24. Nishi, Y. (2009). Integration Challenges and Opportunities of Nanoelectronic Devices. *ECS Transactions.* 25(7), 19-31.
25. Liu, J., Michel, J., Giziewicz, W., Pan, D., Wada, K., Cannon, D. D. and Yasaitis, J. (2005). High-performance, Tensile-strained Ge p-I-n Photodetectors on A Si Platform. *App. Phys. Lett.* 87(10), 493-501.
26. Chen, R. T., Wu, L., Lin, L., Choi, C., Liu, Y., Bihari, B. and Liu, Y. S. (1999). Guided-wave Si CMOS Process-compatible Optical Interconnects. *Am. Soc. Mech. Engs, EEP.* 263, 755-759.
27. Stellari, F., Zappa, F., Cova, S. and Vendrame, L. (2001). Tools for Contactless Testing and Simulation of CMOS Circuits. *Microelect. Rel.* 41(11), 1801-1808.
28. Quevedo, M., Gowrisanker, S., Allee, D., Venugopal, S., Krishna, R., Kaftanoglu, K. and Gnade, B. E. (2009). Novel Materials and Integration Schemes for CMOS-Based Circuits for Flexible Electronics. *ECS Transactions.* 25(7), 503-511.
29. Nam, J. H., Alkis, S., Nam, D., Afshinmanesh, F., Shim, J., Park, J. H. and Saraswat, K. (2015). Lateral Overgrowth of Germanium for Monolithic Integration of Germanium-on-insulator on Silicon. *J. Cryst. Growth.* 416, 21-27.

30. Sawano, K., Hoshi, Y., Endo, S., Nagashima, T., Arimoto, K., Yamanaka, J., Shiraki, Y. (2014). Formation of Ge(111) on Insulator by Ge Epitaxy on Si(111) and Layer Transfer. *Thin Solid Films*. 557, 76-79.
31. Lippert, G., Dabrowski, J., Yamamoto, Y., Herziger, F., Maultzsch, J., Lemme, M. C., Lupina, G. (2013). Molecular Beam Growth of Micrometer-size Graphene on Mica. *Carbon*. 52, 40-48.
32. Seifarth, O., Lippert, G., Dabrowski, J., Lupina, G., Mehr, W. and Lemme, M. C. (2011). Graphene Directly Grown on SiO₂-based Insulators. *Proceedings of the Semiconductor Conference*. 27-28 September. Dresden, Germany, 232-236.
33. Chen, X., Ma, X. C., He, K., Jia, J. F. and Xue, Q. K. (2011). Molecular Beam Epitaxial Growth of Topological Insulators. *Adv. Mater.* 23(9), 1162-1165.
34. Mieda, E., Maeda, T., Miyata, N., Yasuda, T., Kurashima, Y., Maeda, A., Kunii, Y. (2015). Wafer-scale Layer Transfer of GaAs and Ge onto Si Wafers Using Patterned Epitaxial Lift-off. *Japanese Journal of Applied Physics*. 54(3), 436-505.
35. Chia, C. K., Sridhara, A., Suryana, M., Dong, J. R., Wang, B. Z., Dalapati, G. K. and Chi, D. Z. (2008) . GaAs-Ge Materials Integration for Electronic and Photonic Applications. Proceedings of the Group IV Photonics, 2008 5th IEEE International Conference. 17-19 September. Denmark, 221-229.
36. Miura, H., Yasui, K., Abe, K., Masuda, A., Kuroki, Y., Nishiyama, H., Akahane, T. (2008). Epitaxial Growth of SiC on Silicon on Insulator Substrates with Ultrathin Top Si Layer by Hot-Mesh Chemical Vapour Deposition. *Japanese J.App. Phys.* 47(1S), 569-572.
37. Narita, Y., Yasui, K., Eto, J., Kurimoto, T. and Akahane, T. (2005). (100)-Oriented 3C-SiC Polycrystalline Film Grown on SiO₂ by Hot-Mesh Chemical Vapour Deposition Using Monomethylsilane and Hydrogen. *J. J. .App. Phys.* 44(6L), L809.
38. Yasui, K., Miura, H., Eto, J., Narita, Y. and Hashim, A. M. (2010). Heteroepitaxial Growth of SiC at Low Temperatures for the Application of A Pressure Sensor Using Hot-mesh CVD. *Proceedings of the Enabling Science and Nanotechnology (ESciNano)*. 1-3 December. Malaysia, 118-201.

39. Chang, S. J., Bawedin, M., Bayraktaroglu, B., Lee, J. H. and Cristoloveanu, S. (2011). Low-temperature Properties of ZnO on Insulator MOSFETs. *Proceedings of IEEE International SOI*. 3-6 October. Arizona, USA, 1-2.
40. Iwai, H. (1999). CMOS Technology year 2010 and Beyond. *IEEE Sol. Stat. Circ.* 34(3), 357-366.
41. Takagi, S., Zhang, R., Suh, J., Kim, S. H., Yokoyama, M., Nishi, K. and Takenaka, M. (2015). III–V/Ge Channel MOS Device Technologies in Nano CMOS Era. *Japanese Journal of Applied Physics*. 54(6S1), 06FA01.
42. Chae, S. and Lee, Y. (2014). Carbon Nanotubes and Graphene Towards Soft Electronics. *Nano Convergence*. 1(1), 1-26.
43. Jeon, I., Cui, K., Chiba, T., Anisimov, A., Nasibulin, A. G., Kauppinen, E. I. and Matsuo, Y. (2015). Direct and Dry Deposited Single-Walled Carbon Nanotube Films Doped with MoO_x as Electron-Blocking Transparent Electrodes for Flexible Organic Solar Cells. *J. Ams.* 137(25), 7982-7985.
44. Wang, Y., Yang, H. J., Geng, H. Z., Zhang, Z. C., Ding, E. X., Meng, Y. and Da, S. X. (2015). Fabrication and Evaluation of Adhesion Enhanced Flexible Carbon Nanotube Transparent Conducting Films. *J. Mater. Chem. C*. 3(15), 3796-3802.
45. Xia, M., Cheng, Z., Han, J. and Zhang, S. (2014). Extremely Stretchable All-carbon-nanotube Transistor on Flexible and Transparent Substrates. *App. Phys. Lett.* 105(14), 143504.
46. Mali, K. S., Greenwood, J., Adisoejoso, J., Phillipson, R. and De Feyter, S. (2015). Nanostructuring Graphene for Controlled and Reproducible Functionalization. *Nanoscale*. 7(5), 1566-1585.
47. Muszynski R, Seger B andPV, K. (2008). Decorating Graphene Sheets with Gold Nanoparticles. *J. Phys. Chem. C*,. 112(14), 5263-5266.
48. Song, W. T., Xie, J., Liu, S. Y., Zheng, Y. X., Cao, G. S., Zhu, T. J. and Zhao, X. B. (2012). Graphene Decorated with ZnO Nanocrystals with Improved Electrochemical Properties Prepared by a Facile In Situ Hydrothermal Route. *Int. J. Electrochem. Sci.* 7, 2164 - 2174.
49. Bai, H., Li, C. and Shi, G. (2011). Functional Composite Materials Based on Chemically Converted Graphene. *Adv. Mater.* 23(9), 1089-1115.

50. Nguyen, T. P. (2011). Polymer-based Nanocomposites for Organic Optoelectronic Devices. A Review. *Sur. Coat. Tech.* 206(4), 742-752.
51. Ngom, B. D., Sakho, O., Ndiaye, S., Bartali, R., Diallo, A., Gaye, M. B. and Beye, A. C. (2011). Photon-induced Tunable and Reversible Wettability of Pulsed Laser Deposited W-doped ZnO Nanorods. *Euro. Phys. App. Phys.* 55(02), 43-50.
52. Li, Y., Zhao, X., Zhang, P., Ning, J., Li, J., Su, Z. and Wei, G. (2015). A Facile Fabrication of Large-scale Reduced Graphene Oxide-silver Nanoparticle Hybrid Film as A Highly Active Surface-enhanced Raman Scattering Substrate. *J. Mater. Chem. C.* 3(16), 4126-4133.
53. Biroju, R. K., Tilak, N., Rajender, G., Dhara, S. and Giri, P. K. (2015). Catalyst Free Growth of ZnO Nanowires on Graphene and Graphene Oxide and Its Enhanced Photoluminescence and Photoresponse. *Nanotechnology.* 26(14), 145601.
54. Sun, H., Liu, Y., Yu, Y., Ahmad, M., Nan, D. and Zhu, J. (2014). Mesoporous Co₃O₄ Nanosheets 3D-Graphene Networks Hybrid Materials for High Performance Lithium Ion Batteries. *Electro. Chim. Acta.* 118, 1-9.
55. Mendoza-Sánchez, B., Coelho, J., Pokle, A. and Nicolosi, V. (2015). A 2D Graphene-manganese Oxide Nanosheet Hybrid Synthesized by A Single Step Liquid-phase Co-exfoliation Method for Supercapacitor Applications. *Electro. Chim. Acta.* 174, 696-705.
56. Ghosh, D., Giri, S., Moniruzzaman, M., Basu, T., Mandal, M. and Das, C. K. (2014). MnMoO₄/graphene Hybrid Composite: High Energy Density Supercapacitor Electrode Material. *Dalton Trans.* 43(28), 11067-11076.
57. Xie, R., Fan, G., Ma, Q., Yang, L. and Li, F. (2014). Facile Synthesis and Enhanced Catalytic Performance of Graphene-supported Ni Nanocatalyst From A Layered Double Hydroxide-based Composite Precursor. *J. Mater. Chem. A.* 2(21), 7880-7889.
58. Mimouni, R., Kamoun, O., Yumak, A., Mhamdi, A., Boubaker, K., Petkova, P. and Amlouk, M. (2015). Effect of Mn Content on Structural, Optical, Opto-thermal and Electrical Properties of ZnO-Mn Sprayed Thin Films Compounds. *J. Alloy. Compd.* 645, 100-111.

59. Jayaraman, S., Suresh Kumar, P., Mangalaraj, D., Dharmarajan, R., Ramakrishna, S. and P Srinivasan, M. (2015). Gold Nanoparticle Immobilization on ZnO Nanorods via Bi-functional Monolayers: A Facile Method to Tune Interface Properties. *Surf. Sci.* 641, 23-29.
60. Luo, Q., Wu, Z., He, J., Cao, Y., Bhutto, W., Wang, W. and Kang, J. (2015). Facile Synthesis of Composition-tuned ZnO/Zn-x-Cd1-x Se Nanowires for Photovoltaic Applications. *Nanoscale Res. Lett.* 10(1), 1-8.
61. Luo, Q., Wu, Z., He, J., Cao, Y., Bhutto, W. A., Wang, W. and Kang, J. (2015). Facile Synthesis of Composition-tuned ZnO/Zn-x-Cd 2-x Se Nanowires for photovoltaic applications. *Nanoscale Res. Lett.* 10(3), 23-28.
62. Muthulingam, S., Lee, I. H. and Uthirakumar, P. (2015). Highly Efficient Degradation of Dyes by Carbon Quantum Dots/n-doped Zinc Oxide (CQD/N-ZnO) Photocatalyst and Its Compatibility on Three Different Commercial Dyes Under Daylight. *J Coll. Interface Sci.* 455, 101-109.
63. Dang, V. Q., Trung, T. Q., Kim, D. I., Duy, L. T., Hwang, B. U., Lee, D. W. and Lee, N. E. (2015). Ultrahigh Responsivity in Graphene–ZnO Nanorod Hybrid UV Photodetector. *Small.* 11(25), 3054-3065.
64. Zhang, S G., Wen, L., Li, J L., Gao, F L., Zhang, X W., Li, L H. and Li, G Q. (2014). Plasmon-enhanced Ultraviolet Photoluminescence from Highly Ordered ZnO Nanorods/Graphene Hybrid Structure Decorated with Au Nanospheres. *Journal of Physics D: App. Phys.* 47(49), 495103.
65. Nasrin, F., Serge, A. and Paul, A. C. (2014). Fe Doped TiO₂–graphene Nanostructures: Ssynthesis, DFT Modelling and Photocatalysis. *Nanotechnology.* 25(30), 305601-305612.
66. Sousa, S. F., Carvalho, E. S., Ferreira, D. M., Tavares, I. S., Fernandes, P. A., Ramos, M. J. andGomes, J. A. (2009). Comparative Analysis of The Performance of Commonly Available Density Functionals in The Determination of Geometrical Parameters for Zinc Complexes. *J. Comput. Chem.* 30(16), 2752–2763.
67. Ambrožič, G., Škapin, S. D., Žigon, M. andOrel, Z. C. (2010). The synthesis of zinc oxide nanoparticles from zinc acetylacetonate hydrate and 1-butanol or isobutanol. *J. Coll. Interface Sci.* 346(2), 317-323.

68. Musić, S., Šarić, A. and Popović, S. (2010). Formation of Nanosize ZnO Particles by Thermal Decomposition of Zinc Acetylacetonate Monohydrate. *ceram. int.* 36(3), 1117-1123.
69. Ahmad, N. F., Rusli, N. I., Mahmood, M. R., Yasui, K. and Hashim, A. M. (2014). Seed/catalyst-free Ggrowth of Zinc Oxide Nanostructures on Multilayer Graphene by Thermal Evaporation. *Nanoscale Res. Lett.* 9(1), 83-70.
70. Singh, T., Pandya, D. K. and Singh, R. (2012). Surface Plasmon Enhanced Bandgap Emission of Electrochemically Grown ZnO Nanorods Using Au Nanoparticles. *Thin Solid Films.* 520(14), 4646-4649.
71. Chen, W., Zhang, D. W., Ren, J., Lu, H. L., Zhang, J. Y., Xu, M. and Wang, L. K. (2005). Density Functional Theory Study of Initial Stage of ZrO₂ Atomic Layer Deposition on Ge/Si(100)-(2×1) Surface. *Thin Solid Films.* 479(1-2), 73-76.
72. Jung-Hyeun, V. I. ., Thomas, A. and Germer, G. W. Mulholland, Sheryl H. Ehrman. (2003). Co-solvent Assisted Spray Pyrolysis for the Generation of Metal Particles. *J. Mater. Res.* 18(7), 1614–1622.
73. Yu, Z., Tetard, L., Zhai, L. andThomas, J. (2015). Supercapacitor Electrode Materials: Nanostructures From 0 to 3 Dimensions. *Energy Environ. Sci.* 8(3), 702-730.
74. Janotti, A. and Van de Walle, C. G. (2009). Fundamentals of Zinc Oxide as A Semiconductor. *Rep. Prog. Phys.* 72(12), 496-501.
75. Reshchikov, M. A. and Morkoç, H. (2005). Luminescence Properties of Defects in GaN. *J. App. Phys.* 97(6), 613-618.
76. Dai, S., Dunn, M. L. and Park, H. S. (2010). Piezoelectric Constants for ZnO Calculated Using Classical Polarizable Core-shell Potentials. *Nanotechnology.* 21(44), 445-449.
77. Liang-zhi, K., Wan-lin, G. and Li, C. (2008). Piezoelectricity of ZnO and Its Nanostructures. *Proceedings of the conference of the Piezoelectricity, Acoustic Waves and Device Applications SPAWDA.* 5-8 December. China, 354-359.
78. Rodnyi, P. A. and Khodyuk, I. V. (2011). Optical and Luminescence Properties of Zinc Oxide. *Opti. Spect.* 111(5), 776-785.

79. Tharsika, T., Haseeb, A. S., Akbar, S. A., Sabri, M. F. and Hoong, W. Y. (2014). Enhanced Ethanol Gas Sensing Properties of SnO₂-core/ZnO-shell Nanostructures. *Sensors*. 14(8), 14586-14600.
80. Xiao, Q. and Wang, T. (2013). Improving The Ethanol Gas-sensing Properties of Porous ZnO Microspheres by Co-doping. *Mater. Res. Bullet.* 48(8), 2786-2791.
81. Larciprete, M. C., Passeri, D., Michelotti, F., Paoloni, S., Sibilia, C., Bertolotti, M. and Lo Mastro, S. (2005). Second Order Nonlinear Optical Properties of Zinc Oxide Films Deposited by Low Temperature Dual Ion Beam Sputtering. *J. App.Phys.* 97(2), 023501.
82. Kroetch, A. (2009). Fabrication of Nonlinear Optical Devices in Ionically Self-Assembled Monolayers. *J. MEMS. MOEMS.* 8(1), 013011.
83. Novoselov, K. S., Geim, A. K., Morozov, S. V., Jiang, D., Zhang, Y., Dubonos, S. V. and Firsov, A. A. (2004). Electric Field Effect In Atomically Thin Carbon Films. *Science*. 306(5696), 666-669.
84. Balandin, A. A., Ghosh, S., Bao, W., Calizo, I., Teweldebrhan, D., Miao, F. and Lau, C. N. (2008). Superior Thermal Conductivity of Single-layer Graphene. *Nano Lett.* 8(3), 902-907.
85. Kim, K. S., Zhao, Y., Jang, H., Lee, S. Y., Kim, J. M., Kim, K. S. and Hong, B. H. (2009). Large-scale Pattern growth of Graphene Films for Stretchable Transparent Electrodes. *Nature*. 457(7230), 706-710.
86. Novoselov, K. S., Geim, A. K., Morozov, S. V., Jiang, D., Katsnelson, M. I., Grigorieva, I. V. and Firsov, A. A. (2005). Two-dimensional Gas of Massless Dirac Fermions in Graphene. *Nature*. 438(7065), 197-200.
87. Zhang, Y., Tan, Y. W., Stormer, H. L. and Kim, P. (2005). Experimental Observation of The Quantum Hall Effect and Berry's Phase in Graphene. *Nature*. 438(7065), 201-204.
88. Basu, S. and Bhattacharyya, P. (2012). Recent Developments on Graphene and Graphene Oxide Based Solid State Gas Sensors. *Sensor. Actuat. B:Chem.* 173, 1-21.
89. Reich, S., Maultzsch, J., Thomsen, C. and Ordejón, P. (2002). Tight-binding Description of Graphene. *Phy.s Rev. B.* 66(3), 832-837.

90. Zulhasan, K. (2012). *Graphene and ZnO Nanostructures for Nano-Optoelectronic, Biosensing Applications*. Doctor of Philosophy, Linköping University, Sweden.
91. Kim, Y. J., Hadiyawarman, Yoon, A., Kim, M., Yi, G. C. and Liu, C. (2011). Hydrothermally Grown ZnO Nanostructures on Few-layer Graphene Sheets. *Nanotechnology*. 22(24), 245603 (245601-245608).
92. Kim, Y. J., Yoo, H., Lee, C. H., Park, J. B., Baek, H., Kim, M. and Yi, G. C. (2012). Position and Morphology Controlled ZnO Nanostructures Grown on Graphene Layers. *Adv. Mater.* 24(41), 5565-5569.
93. Yi, J., Lee, J. M. and Park, W. I. (2011). Vertically Aligned ZnO Nanorods and Graphene Hybrid Architectures for High-sensitive Flexible Gas Sensors. *Sensor. Actuat. B. Chem.* 155(1), 264-269.
94. Liu, J. y., Yu, X., Zhang, G. H., Wu, Y. K., Zhang, K., Pan, N. and Wang, X. P. (2013). High Performance Ultraviolet Photodetector Fabricated with ZnO Nanoparticles Graphene Hybrid Structures. *Chin. J. Chem. Phys.* 26(2), 225-230.
95. Waugh, M. R., Hyett, G. and Parkin, I. P. (2008). Zinc Oxide Thin Films Grown by Aerosol Assisted CVD. *Chem. Vap. Depos.* 14(11-12), 366-372.
96. Lehraki, N., Aida, M. S., Abed, S., Attaf, N., Attaf, A. and Poulain, M. (2012). ZnO thin films deposition by spray pyrolysis: Influence of Precursor Solution Properties. *Curr. App. Phys.* 12(5), 1283-1287.
97. Sandana, V. E., Rogers, D. J., Hosseini Teherani, F., McClintock, R., Bayram, C., Razeghi, M. and Falyouni, F. (2009). Comparison of ZnO Nanostructures Grown Using Pulsed Laser Deposition, Metal Organic Chemical Vapour Deposition and Physical Vapour Transport. *J. Vac. Sci. e . Tech. B.* 27(3), 1678-1683.
98. Prestgard, M. C., Siegel, G., Roundy, R., Raikh, M. and Tiwari, A. (2015). Temperature Dependence of The Spin Relaxation in Highly Degenerate ZnO Thin Films. *J. App. Phys.* 117(8), 883-905.
99. Xu, Q., Zhou, S., Markó, D., Potzger, K., Fassbender, J., Vinnichenko, M. and Schmidt, H. (2009). Paramagnetism in Co-doped ZnO Films. *J. Phys D: App. Phys.* 42(8), 485-501.

100. Jang, J. H., Kim, H. S., Norton, D. P. and Craciun, V. (2009). Study of Microstructural Evolutions in Phosphorus Doped ZnO Films Grown by Pulsed Laser Deposition. *J. Cryst. Growth.* 311(11), 3143-3146.
101. Yu, W., Zhang, L., Zhang, Z. C., Yang, L. H., Teng, X. Y., Zhang, J. C. and Fu, G. S. (2009). Structural and Ferromagnetic Characteristics of ZnO-Mn Thin Films. *J. Synth. Cryst.* 38(3), 685-688.
102. Chen, Z., Shum, K., Salagaj, T., Wei, Z. and Strobl, K. (2010). ZnO Thin Films Synthesized by Chemical Vapour Deposition. *Proceedings of the Long Island Systems Applications and Technology Conference (LISAT)*. 7-8 May. Farmingdale State, USA, 1-5.
103. Teng, X. M., Fan, H. T., Pan, S. S., Ye, C. and Li, G. H. (2006). Photoluminescence of ZnO Thin Films on Si Substrate with and without ITO Buffer Layer. *J. Phys D: App. Phys.* 39(3), 471-476.
104. Zhao, G. L., Lin, B. X., Hong, L., Meng, X. D. and Fu, Z. X. (2004). Structural and Luminescent Properties of ZnO Thin Films Deposited by Atmospheric Pressure Chemical Vapour Deposition. *Chin. Phys. Lett.* 21(7), 1381-1384.
105. Fan, D., Zhang, R., Wang, X., Huang, S. and Peng, H. (2012). Influence of Silver Dopant on The Morphology and Ultraviolet Emission in Aligned ZnO Nanostructures. *Physi. Stat. solidi (a)*. 209(2), 335-339.
106. Alvarado, J. A., Maldonado, A., Juarez, H., Pacio, M. and Perez, R. (2015). Characterization of Nanostructured ZnO Thin Films Deposited Through Vacuum Evaporation. *Beilst. J. Nanotech.* 6, 971-975.
107. Fawzy A.Mahmoud, G. K. Nanocrystalline ZnO Thin Film for Gas Sensor Application. *J. Ovonic Res.* 5(1), 15-20.
108. Della Gaspera, E., Guglielmi, M., Perotto, G., Agnoli, S., Granozzi, G., Post, M. L. and Martucci, A. (2012). CO Optical Sensing Properties of Nanocrystalline ZnO–Au Films: Effect of Doping With Transition Metal Ions. *Sensor. Actu. B: Chem.* 161(1), 675-683.
109. Mahalingam, T. and Hsu, L.S. (2007). Microstructural Analysis of Electrodeposited Zinc Oxide Thin Films. *J. New Mater. Elect. Sys.* 10, 9-14.

110. Chang, C. J., Hsu, M. H., Weng, Y. C., Tsay, C. Y. and Lin, C. K. (2013). Hierarchical ZnO Nanorod-array Films With Enhanced Photocatalytic Performance. *Thin Solid Films*. 528, 167-174.
111. Ahmad, N. F., Rusli, N. I., Mahmood, M. R., Yasui, K. and Hashim, A. M. (2014). Seed/Catalyst Free Growth of Zinc Oxide Nanostructures on Multilayer Graphene by Thermal Evaporation. *Nano. Res Lett*. 9(1), 83-92.
112. Jiao, S., Zhang, K., Bai, S., Li, H., Gao, S., Li, H. and Zhao, L. (2013). Controlled Morphology Evolution of ZnO Nanostructures in The Electrochemical Deposition: From The Point of View of Chloride Ions. *Electrochimica Acta*. 111, 64-70.
113. Hilder, M., Winther-Jensen, O., Winther-Jensen, B. and MacFarlane, D. R. (2012). Graphene/Zinc Nano-composites by Electrochemical Co-deposition. *Phys. Chem. Chem. Phys.* 14(40), 14034–14040.
114. Damm, H., Kelchtermans, A., Bertha, A., Van den Broeck, F., Elen, K., Martins, J. C. and Van Bael, M. K. (2013). Thermal Decomposition Synthesis of Al-doped ZnO Nanoparticles: An In-depth Study. *RSC Advances*. 3(45), 23745-23751.
115. Ghaffarian, H. R., Mahboobeh, S. and Sayyadnejad, M. A. (2011). Synthesis of ZnO Nanoparticles by Spray Pyrolysis Method. *Iran. J. Chem. Chem. Eng.* 30(1), 1-6.
116. Agouram, S., Bushiri, M. J., Montenegro, D. N., Reig, C., Martínez-Tomás, M. C. and Muñoz-Sanjosé, V. (2012). Synthesis and Characterization of ZnO Nano and Micro Structures Grown by Low Temperature Spray Pyrolysis and Vapour Transport. *J. f Nanosci. Nanotech.* 12(8), 6792-6799.
117. Wallace, R., Brown, A. P., Brydson, R., Wegner, K. and Milne, S. J. (2013). Synthesis of ZnO Nanoparticles by Flame Spray Pyrolysis and Characterisation Protocol. *J. Mater Sci.* 48(18), 6393-6403.
118. Aziz, N. S. A., Nishiyama, T., Rusli, N. I., Mahmood, M. R., Yasui, K. and Hashim, A. M. (2014). Seedless Growth of Zinc Oxide Flower-shaped Structures on Multilayer Graphene by Electrochemical Deposition. *Nanoscale Res. Lett.* 9(1), 337-346.
119. Aziz, N. S. A., Mahmood, M. R., Yasui, K. and Hashim, A. M. (2014). Seed/Catalyst-free Vertical Growth of High Density Electrodeposited Zinc

- Oxide Nanostructures on A Single Layer Graphene. *Nanoscale Res. Lett.* 9, 95-102.
120. Choi, W. M., Shin, K. S., Lee, H. S., Choi, D., Kim, K., Shin, H. J. and Kim, S. W. (2011). Selective Growth of ZnO Nanorods on SiO₂/Si Substrates Using Graphene Buffer Layer. *Nano Res.* 4(5), 440-447.
 121. Karber, E., Raadik, T., Dedova, T., Krustok, J., Mere, A., Mikli, V. and Krunks, M. (2011). Photoluminescence of Spray Pyrolysis Deposited ZnO Nanorods. *Nanoscale Res Lett.* 6(1), 359-368.
 122. Liu, P., Li, Y., Guo, Y. and Zhang, Z. (2012). Growth of Catalyst-free High Quality ZnO Nanowires by Thermal Evaporation Under Air Ambient. *Nanoscale Res. Lett.* 7(3), 442-449.
 123. Opoku, C., Hoettges, K. F., Hughes, M. P., Stolojan, V., Silva, S. R. P. and Shkunov, M. (2013). Solution Processable Multi-channel ZnO Nanowire Field Effect Transistors With Organic Gate Dielectric. *Nanotechnology.* 24(40), 405-409.
 124. Öztürk, S., Kılınç, N., Taşaltın, N. and Öztürk, Z. Z. (2012). Fabrication of ZnO Nanowires and Nanorods. *Physica E: Low dim. Sys. Nanost.* 44(6), 1062-1065.
 125. Öztürk, S., Kılınç, N., Taşaltın, N. and Öztürk, Z. Z. (2011). A Comparative Study on The NO₂ Gas Sensing Properties of ZnO Thin Films, Nanowires and Nanorods. *Thin Solid Films.* 520(3), 932-938.
 126. Shrama, S. K., Saurakhiya, N., Barthwal, S., Kumar, R. and Sharma, A. (2014). Tuning of Structural, Optical and Magnetic Properties of Ultrathin and Thin ZnO Nanowire Arrays for Nano-device Applications. *Nanoscale Res. Lett.* 9(1), 102-107.
 127. Bu, I. Y. (2014). Optoelectronic Properties of ZnO Nanowires Deposited Under Different Zinc Nitrate/Hexamine Ratio Concentrations. *Ceram. Int.* 40(4), 6345-6350.
 128. Htay, M. T. and Hashimoto, Y. (2015). Field Emission Property of ZnO Nanowires Prepared by Ultrasonic Spray Pyrolysis. *Superlatt. Microst.* 84, 144-153.

129. Breedon, M., Rahmani, M. B., Keshmiri, S. H., Wlodarski, W. and Kalantar Z. (2010). Aqueous Synthesis of Interconnected ZnO Nanowires Using Spray Pyrolysis Deposited Seed Layers. *Mater. Lett.* 64(3), 291-294.
130. Farooq, R., Mahmood, T., Anwar, A. W., and Abbasi, G. N. (2016). First Principles Calculation of Electronic and Optical Properties of Graphene Like ZnO (G-ZnO). *Superlat. and Microstruct.* 90, 165-169.
131. Pruna, A., Shao, Q., Kamruzzaman, M., Zapien, J. A., and Ruotolo, A. (2016). Enhanced Electrochemical Performance of ZnO Nanorod Core/Polypyrrole Shell Arrays by Graphene Oxide. *Electrochim. Act.* 187, 517-524.
132. Utama, M. I. B., Zhang, J., Chen, R., Xu, X., Li, D., Sun, H. and Xiong, Q. (2012). Synthesis and Optical Properties of II–VI 1D Nanostructures. *Nanoscale.* 4(5), 1422–1435.
133. Liu, L., Ryu, S., Tomasik, M. R., Stolyarova, E., Jung, N., Hybertsen, M. S. and Flynn, G. W. (2008). Graphene Oxidation: Thickness Dependent Etching and Strong Chemical Doping. *Nano Lett.* 8(7), 1965-1970.
134. Ahmad, N. F., Rusli, N. I., Mahmood, M. R., Yasui, K. and Hashim, A. M. (2014). Seed/Catalyst-free Growth of Zinc Oxide Nanostructures on Multilayer Graphene by Thermal Evaporation. *Nanoscale Res. Lett.* 9(1), 81-87.
135. Astuti, B., Tanikawa, M., Rahman, S. F. A., Yasui, K. and Hashim, A. M. (2012). Graphene as A Buffer Layer for Silicon Carbide on Insulator Structures. *Materials.* 5(12), 2270-2279.
136. Bekermann, D., Ludwig, A., Toader, T., Maccato, C., Barreca, D., Gasparotto, A. and Devi, A. (2011). MOCVD of ZnO Films From Bis(Ketoiminato)Zn(II) Precursors: Structure, Morphology and Optical Properties. *Chem. Vap. Depos.* 17(4-6), 155-161.
137. Choy, K. L. (2003). Chemical Vapour Deposition of Coatings. *Progress in Mater Sci.* 48, 57–170.
138. Dainius P. and Gauckler, L. J. (2005). Thin Film Deposition Using Spray Pyrolysis. *J. Electroceramics.* 14(14), 103-111.

139. Mwakikunga, B. W. (2013). Progress in Ultrasonic Spray Pyrolysis for Condensed Matter Sciences Developed From Ultrasonic Nebulization Theories Since Michael Faraday. *Crit. Rev. Solid state Mat. Sci.* 39(1), 46-80.
140. Scarisoreanu, M., Morjan, Alexandrescu, R., Birjega, R., Voicu, I., Fleaca, C. and Figgemeier, E. (2007). Effects of Some Synthesis Parameters on The Structure of Titania Nanoparticles Obtained by Laser Pyrolysis. *App. Surf. Sci.* 253(19), 7908-7911.
141. Mwakikunga, B. W., Forbes, A., Sideras, H. E. and Arendse, C. (2008). Optimization, Yield Studies and Morphology of WO₃ Nano-Wires Synthesized by Laser Pyrolysis in C₂H₂ and O₂ Ambients—Validation of a New Growth Mechanism. *Nanoscale Res. Lett.* 3(10), 372-380.
142. Sirignano, B. A. a. W. A. (1989). Droplet Vaporization Model for Spray Combustion Calculations. *International Journal of Heat and Mass Transfer.* 32(9), 1605-1618.
143. Jayah, N., Yahaya, H., Mahmood, M., Terasako, T., Yasui, K. and Hashim, A. (2015). High Electron Mobility and Low Carrier Concentration of Hydrothermally Grown ZnO Thin Films on Seeded a-plane Sapphire at Low Temperature. *Nanoscale Research Letters.* 10(1), 1-10.
144. Tak, Y. and Yong, K. (2005). Controlled Growth of Well-aligned ZnO Nanorod Array Using A Novel Solution Method. *J. Phys. Chem. B.* 109(41), 19263-19269.
145. Chen, H. G., Lian, H. D., Hung, S. P. and Wang, C. F. (2013). Epitaxial Growth of Self-ordered ZnO Nanostructures on Sapphire Substrates by Seed-Assisted Hydrothermal Growth. *J. Cryst. Growth.* 362, 231-234.
146. Choi, H. S., Vaseem, M., Kim, S. G., Im, Y. H. and Hahn, Y. B. (2012). Growth of High Aspect Ratio ZnO Nanorods by Solution Process: Effect of Polyethyleneimine. *J. Solid State Chem.* 189, 25-31.
147. Guo, M., Diao, P. and Cai, S. (2005). Hydrothermal Growth of Well-aligned ZnO Nanorod arrays: Dependence of Morphology and Alignment Ordering Upon Preparing Conditions. *J. Solid State Chem.* 178(6), 1864-1873.
148. Aziz, N. S. A., Mahmood, M. R., Yasui, K. and Hashim, A. M. (2014). Seed/Catalyst-free Vertical Growth of High Density Electrochemically

- Deposited Zinc Oxide Nanostructures on a Single Layer Graphene. *Nanoscale Res. Lett.* 9(1), 95 (91-97).
149. Xu, C., Lee, J. H., Lee, J. C., Kim, B. S., Hwang, S. W. and Whang, D. (2011). Electrochemical Growth of Vertically Aligned ZnO Nanorod Arrays on Oxidized Bi-layer Graphene Electrode. *Cryst. Eng. Comm.* 13(20), 6036-6039.
 150. Yuan, F.L., Kelder, E.M. and J. Schoonman. (1998). Preparation of Zirconia and Yttria-stabilized Zirconia (YSZ) Fine Powders by Flame Assisted Ultrasonic Spray Pyrolysis (FAUSP). *Solid State Ionics.* 109(109), 119-123.
 151. Lee, D. Y. and Kim, J. (2011). Deposition of CuInS₂ Films by Electrostatic Field Assisted Ultrasonic Spray Pyrolysis. *Sol. Energ. Mat. Sol. C.* 95(1), 245-249.
 152. Ksapabutr, B., Nimnuan, P. and Panapoy, M. (2015). Dense and Uniform NiO Thin Films Fabricated by One-step Electrostatic Spray Deposition. *Mater. Lett.* 153, 24-28.
 153. Ksapabutr, B., Pongchun, G. and Panapoy, M. (2010). Architectural Control of ZrO₂ thin Films Via The Electrostatic Spray Deposition Technique Using Zirconatane as A Precursor. *Phys.Scr.* T(139), 140-145.
 154. Curcio, F. and Notaro, N. (1990). Synthesis of Ultrafine TiO₂ Powders by A CW CO₂ Laser. *App. Surf. Sci.* 46(46), 225-229.
 155. Veintemillas, V. S., Morales, P., Di Nunzio, P. E. and Martelli, S. (2003). Iron Ultrafine Nanoparticles Prepared by Aerosol Laser Pyrolysis. *Mater. Lett.* 57, 1184–1189.
 156. Goto, T., Banal, R. and Kimura, T. (2007). Morphology and Preferred Orientation of Y₂O₃ Film Prepared by High-speed Laser CVD. *Surf. Coat. Tech.* 201(12), 5776-5781.
 157. Dhonge, B. P., Mathews, T., Tripura Sundari, S., Krishnan, R., Balamurugan, A. K., Kamruddin, M. and Tyagi, A. K. (2013). Synthesis of Al₂O₃ Thin Films Using Laser Assisted Spray Pyrolysis (LASP). *App. Surf. Sci.* 265, 257-263.
 158. Wallace, R., Brown, A. P., Brydson, R., Wegner, K. and Milne, S. J. (2013). Synthesis of ZnO Nanoparticles by Flame Spray Pyrolysis and Characterisation Protocol. *J. Mater. Sci.* 48(18), 6393-6403.

159. Arutanti, O., Nandiyanto, A. B. D., Ogi, T., Iskandar, F., Kim, T. O. and Okuyama, K. (2014). Synthesis of Composite WO₃/TiO₂ Nanoparticles by Flame-assisted Spray Pyrolysis and Their Photocatalytic Activity. *J. Alloy. Compd.* 591, 121-126.
160. Becke, A. D. (2014). Perspective: Fifty Years of Density-Functional Theory in Chemical Physics. *J. Chem. Phys.* 140(18), 301-319.
161. Ruzsinszky, A. and Perdew, J. P. (2011). Twelve Outstanding Problems in Ground-State Density Functional Theory: A Bouquet of Puzzles. *Comput. l Theor. Chem.* 963(1), 2-6.
162. Bader, R. F. W. (2010). The Density in Density Functional Theory. *Theo.Chem.* 943(1-3), 2-18.
163. Perdew, J. P. (2010). Commentary on "The Most-Cited Physicists of The Past 30 Years" and "The Leadership Role of Density Functional Theory". Tulane University, New Orleans.
164. Becke, A. D. (2009). A Density-Functional Approximation for Relativistic Kinetic Energy. *J. Chem. Phys.* 131(24), 244118-244123.
165. Becke, A. D. (1993). Density-Functional Thermochemistry. III. The Role of Exact Exchange. *J. Chem. Phys.* 98(7), 5648-5652.
166. Raghavachari, K. (2000). Perspective on "Density Functional Thermochemistry. III. The Role of Exact Exchange". *Theor. Chem. Acc.* 103(3-4), 361-363.
167. Perdew, J. P., Ruzsinszky, A., Constantin, L. A., Sun, J. and Csonka, G. b. I. (2009). Some Fundamental Issues in Ground-state density functional t: A Guide for The Perplexed. *J. Chem. Theor. Comput.* 5(4), 902-908.
168. Schmider, H. L. and Becke, A. D. (1998). Density Functionals From The Extended G2 Test Set: Second-Order Gradient Corrections. *J. Chem. Phys.* 109(19), 8188-8199.
169. Pederson, M. R., Ruzsinszky, A. and Perdew, J. P. (2014). Communication: Self-Interaction Correction With Unitary Invariance in Density Functional Theory. *J. Chem. Phys.* 140(12), 121103-121103.
170. Schmider, H. L. and Becke, A. D. (1998). Optimized Density Functionals from The Extended G2 Test Set. *J. Chem. Phys.* 108(23), 9624-9631.

171. Hertwig, R. H. and Koch, W. (1997). On The Parameterization of The Local Correlation Functional. What Is Becke-3-LYP?. *Chem. Phys. Lett.* 268(5-6), 345-351.
172. Yanai, T., Tew, D. P. and Handy, N. C. (2004). A New Hybrid Exchange–Correlation Functional Using The Coulomb-Attenuating Method (CAM-B3LYP). *Chem. Phys. Lett.* 393(1-3), 51-57.
173. Zhu, W., Liu, X.-Q., Hou, X., Chen, J., Kim, C. K. and Xu, K. (2014). Modelling of Catalytically Oxidative Decomposition of Carbon Tetrachloride on A ZnS Nanocluster Using Density Functional Theory. *Catal. Sci. Tech.* 4(4), 1038.
174. Shen, Y., Meng, Q., Huang, S., Wang, S., Gong, J. and Ma, X. (2012). Reaction Mechanism of Dimethyl Carbonate Synthesis on Cu/ β Zeolites: DFT and AIM Investigations. *RSC Advances.* 2(18), 7109.
175. Smith, S.M. and Schlegel, B. (2003). Molecular Orbital Studies of Zinc Oxide Chemical Vapour Deposition: Gas-Phase Hydrolysis of Diethyl Zinc, Elimination Reactions and Formation of Dimers and Tetramersf. *Chem. Mater.* 15(1), 162-166.
176. Munk, B. and Schlegel, B. (2006). Molecular Orbital Studies of Zinc Oxide Chemical Vapour Deposition: Gas-Phase Radical Reactions. *Chem. Mater.* 18(7), 1878-1884.
177. Duward Shriver, M. W., Tina Overton, Fraser Armstrong, Jonathan Rourke (2014). d-Metal organometallic. chemistry *Inorganic Chemistry.* 6th, 634-654. United Kingdom: macmillan education.
178. Peter, A. (2014). Physical Chemistry Thermodynamics, Structure and Change. United Kingdom: macmillan education.
179. Becke, A. D. (1992). Density-Functional Thermochemistry. II. The Effect of The Perdew-Wang Generalized-Gradient Correlation Correction. *J. Chem. Phys.* 97(12), 9173-9177.
180. Adejoro, I., Oyeneyin, O. and Obaleye, J. A. (2013). Characterization of A Novel Polymeric Zinc (II) Complex Containing The Anti-Malarial Quinine as Ligand: A Theoretical Approach (Semi-empirical and DFT methods). *Am. J. Sci. Ind. Res.,* 4(1), 111-122.

181. Hehre, W. J. (2003). Theoretical Models. *A Guide to Molecular Mechanics and Quantum Chemical Calculations* (pp. 385-445). Canada Wavefunction, Inc.
182. Dixon, D. A., Dunning, T. H., Eades, R. A. and Gassman, P. G. (1983). Generalized Valence Bond Description of Simple Ylides. *J. Am. Chem. Soc.* 105(24), 7011-7017.
183. Hehre, W. J. (2003). Graphical Models *A Guide to Molecular Mechanics and Quantum Chemical Calculations* (pp. 61-88). Canada: Wavefunction, Inc.
184. Urzay, J., Sánchez, L., Liñan, L. and Williams, F. A. (2013). Flamelet Structures in Spray Ignition. Stanford University, USA.
185. Abramzon, B. and Williams, A. S. (1989). Droplet Vaporization Model for Spray Combustion Calculations. *Int. J. Heat Mass Transfer.* 32(9), 1605-1618.
186. International Organization for Standardization (2008). *ISO/TS 27687:2008*. USA: International Organization for Standardization.
187. Olson, E. (2011). Shape Factors and Their Use in Image Analysis—Part 1: Theory. *J. GXP Compl.* 15(3), 85-96.
188. Dalmoro, A., Barba, A. A. and D'Amore, M. (2013). Analysis of Size Correlations for Microdroplets Produced by Ultrasonic Atomization. *Sci. World J.* 2013, 7-14.
189. Dalmoro, A., d'Amore, M. and Barba, A. A. (2013). Droplet Size Prediction in The Production of Drug Delivery Microsystems by Ultrasonic Atomization. *Transl. Medi. UniSa.* 7, 6-11.
190. Rajan, R. and Pandit, A. B. (2001). Correlations to Predict Droplet Size in Ultrasonic Atomisation. *Ultrasonics.* 39(4), 235-255.
191. Goncalves, G., Marques, P. A., Granadeiro, C. M., Nogueira, H., Singh, M. K. and Grácio, J. (2009). Surface Modification of Graphene Nanosheets with Gold Nanoparticles: The Role of Oxygen Moieties at Graphene Surface on Gold Nucleation and Growth. *Chem. Mater.* 21(20), 4796-4802.
192. Rani, J. R., Lim, J., Oh, J., Kim, J. W., Shin, H. S., Kim, J. H. and Jun, S. C. (2012). Epoxy to Carbonyl Group Conversion in Graphene Oxide Thin Films: Effect on Structural and Luminescent Characteristics. *J. Phys. Chem. C.* 116(35), 19010-19017.

193. Rudolph, G., and Henry, M. C. (1964). The Thermal Decomposition of Zinc Acetylacetonate Hydrate. *Inorgan. Chem.* 3(9), 1317-1318.
194. Kim, Y. J., Hadiyawarman, Yoon, A., Kim, M., Yi, G. C. and Liu, C. (2011). Hydrothermally Grown ZnO Nanostructures on Few-layer Graphene Sheets. *Nanotechnology.* 22(24), 245603-245611.
195. Kim, Y. J., Yoo, H., Lee, C. H., Park, J. B., Baek, H., Kim, M. and Yi, G. C. (2012). Position and Morphology-controlled ZnO Nanostructures Grown on Graphene Layers. *Adv. Mater.* 24(41), 5565-5570.
196. Yan, L., Zheng, Y. B., Zhao, F., Li, S., Gao, X., Xu, B. and Zhao, Y. (2012). Chemistry and pPhysics of A Single Atomic Layer: Strategies and Challenges for Functionalization of Graphene and Graphene-based Materials. *Chem. Soc. Rev.* 41(1), 97-114.
197. Xiang, Q., Yu, J. and Jaroniec, M. (2012). Graphene-based Semiconductor Photocatalysts. *Chem. Soc. Rev.* 41(2), 782-796.
198. Lee, J. M., Pyun, Y. B., Yi, J., Choung, J. W. and Park, W. I. (2009). ZnO Nanorod-graphene Hybrid Architectures for Multifunctional Conductors. *Phys. Chem. C.* 113(44), 19134-19138.
199. Nguyen, N. K. and Borkowski, J. J. (2008). New 3-level Response Surface Designs Constructed From Incomplete Block Designs. *J. Statist. Plann. Infer.* 138(1), 294-305.
200. Nicolai, R. P., Dekker, R., Piersma, N. and Van Oortmarssen, G. J. (2004). Automated Response surface methodology for Stochastic Optimization Models with Unknown Variance. *Proceedings of the 2004 Winter Simulation Conference.* 12-15 January. Netharlands, 492-499.
201. Vining, G. G. and Kowalski, S. (2011). Introduction to Response Surface Methodology. *Statistical Methods for Engineers* (pp. 548-578). united states: Cengage Learning.
202. Lenth, R. V. (2009). Response-surface Methods in R, Using RSM. *J. Statist. Software.* 32(7), 1-17.
203. Sinclair, W., Leane, M., Clarke, G., Dennis, A., Tobyn, M. and Timmins, P. (2011). Physical Stability and Recrystallization Kinetics of Amorphous Ibipinabant Drug Product by Fourier Transform Raman Spectroscopy. *J. Pharm. Sci.* 100(11), 4687-4699.

204. Málek, J. and Mitsuhashi, T. (2000). Testing Method for The Johnson-Mehl-Avrami Equation in Kinetic Analysis of Crystallization Processes. *J. Am. Ceram.* 83(8), 2103-2105.
205. Ayouchi, R., Martin, F., Leinen, D. and Ramos-Barrado, J. R. (2003). Growth of Pure ZnO Thin Films Prepared by Chemical Spray Pyrolysis on Silicon. *J. Cryst. Growth.* 247(3-4), 497-504.
206. Marangoni, A. (1998). On The Use and Misuse of The Avrami Equation in Characterization of The Kinetics of Fat Crystallization. *J. Am. Oil Chem. Soc.* 75(10), 1465-1467.
207. Shi, Z. F., Zhang, Y. T., Cai, X. P., Wang, H., Wu, B., Zhang, J. X. and Du, G. T. (2014). Parametric Study on The Controllable Growth of ZnO Nanostructures with Tunable Dimensions Using Catalyst-free Metal Organic Chemical Vapour Deposition. *Cryst. Eng. Comm.* 16(3), 455-463.
208. Wallace, A. R. (1869). *The Malay Archipelago: The Land of the Orang-utan and the Bird of Paradise; A Narrative of Travel, with Studies of Man and Nature*. Dover Publications: United kingdom.
209. Scholes-Iii, E. (2008). Evolution of The Courtship Phenotype in The Bird of Paradise Genus Parotia (Aves: Paradisaeidae): Homology, Phylogeny and Modularity. *Bio. J. Linnean Soc.* 94(3), 491-504.
210. Lv, Y., Yu, L., Huang, H., Feng, Y., Chen, D. and Xie, X. (2012). Application of The Soluble Salt-Assisted Route to Scalable Synthesis of ZnO Nanopowder with Repeated Photocatalytic Activity. *Nanotechnology.* 23(6), 385-402.
211. Emerson A. ., Luis, V. A. and Viviany, G. (2010). Evaluation of Bulk and Surfaces Absorption Edge Energy of Sol-Gel-Dip-Coating SnO₂ Thin Films. *Mater. Res.* 13(4), 437-443.
212. Wang, T., Jiao, Z., Chen, T., Li, Y., Ren, W., Lin, S. and Bi, Y. (2013). Vertically Aligned ZnO Nanowire Arrays Tip-grafted with Silver Nanoparticles for Photoelectrochemical Applications. *Nanoscale.* 5(16), 7552-7557.
213. Hwang, J. O., Lee, D. H., Kim, J. Y., Han, T. H., Kim, B. H., Park, M. and Kim, S. O. (2011). Vertical ZnO Nanowires/Graphene Hybrids for Transparent and Flexible Field Emission. *J. Mater. Chem.* 21(10), 3432-3437.

214. Guisheng Li, D. Z. a. J. C. Y. (2009). Thermally Stable Ordered Mesoporous CeO₂/TiO₂ Visible-Light Photocatalysts. *Phys. Chem. Chem. Phys.* 11, 3775–3782.
215. Özgu, H. M. a. Ü. (2009). General Properties of ZnO *Zinc Oxide: Fundamentals, Materials and Device Technology* (pp. 1-76). Weinheim: WILEY-VCH Verlag.
216. Ivill, M., Pearton, S. J., Rawal, S., Leu, L., Sadik, P., Das, R. and Norton, D. P. (2008). Structure and Magnetism of Cobalt-doped ZnO Thin Films. *New J. Phys.* 10(6), 765-772.
217. Wang, X., Liu, Y., Zhou, X., Li, B., Wang, H., Zhao, W. and Shen, H. (2012). Synthesis of Long TiO₂ Nanowire Arrays with High Surface Areas Via Synergistic Assembly Route for Highly Efficient Dye-sensitized Solar Cells. *J. Mater. Chem.* 22(34), 17531-17539.
218. Archana, P. S., Naveen Kumar, E., Vijila, C., Ramakrishna, S., Yusoff, M. M. and Jose, R. (2013). Random Nanowires of Nickel Doped TiO₂ with High Surface Area and Electron Mobility for High Efficiency Dye-Sensitized Solar Cells. *Dalton Trans.* 42(4), 1024-1032.
219. Wei-Qing, L., Zhong, G. L., Dong, K., Lin-Hua, H. and Song, Y. D. (2013). Wide Frequency Range Diagnostic Impedance Behavior of The Multiple Interfaces Charge Transport and Transfer Processes in Dye-sensitized Solar Cells. *Electrochimica Acta.* 88, 395-403.
220. Faia, P. M., Furtado, C. S. and Ferreira, A. J. (2005). AC Impedance Spectroscopy: A New Equivalent Circuit for Titania Thick Film Humidity Sensors. *Sensor. Actu. B: Chemical.* 107(1), 353-359.
221. Zhang, L. L. and Zhao, X. S. (2009). Carbon-based Materials as Supercapacitor Electrodes. *Chem. Soc. Rev.* 38(9), 2520-2531.
222. Sparreboom, W., van den Berg, A. and Eijkel, J. C. T. (2010). Transport in Nanofluidic Systems: A Review of Theory and Applications. *New J. Phys.* 12(1), 115-117.
223. Liu, R., Duay, J. and Lee, S. B. (2011). Heterogeneous Nanostructured Electrode Materials for Electrochemical Energy Storage. *Chem. Commun. (Camb).* 47(5), 1384-1404.

224. Molins, S., Trebotich, D., Steefel, C. I. and Shen, C. (2012). An Investigation of The Effect of Pore Scale Flow on Average Geochemical Reaction Rates Using Direct Numerical Simulation. *Wat. Resources Res.* 48(3), 242-250.
225. Meland, A. K., Bedeaux, D. and Kjelstrup, S. (2005). A Gerischer Phase Element in The Impedance Diagram of The Polymer Electrolyte Membrane Fuel Cell Anode. *J.Phys. Chem. B.* 109(45), 21380-21388.
226. Bargteil, D. and Solomon, T. (2012). Barriers to Front Propagation in Ordered and Disordered Vortex Flows. *Chaos.* 22(3), 73-103.
227. Zuo, P. and Zhao, Y. P. (2015). A Phase Field Model Coupling Lithium Diffusion and Stress Evolution with Crack Propagation and Application in Lithium Ion Batteries. *Phys. Chem. Chem. Phys.* 17(1), 287-297.

APPENDIX A

Publications Related to this work

1. **Amgad Ahmed Ali Ibrahim**, Abdul Manaf Hashim, “Density Functional Theory Study of Atomic Layer Deposition of Zinc Oxide on Graphene”, *Nanoscale Res Lett*, 2015. 10:299. (Impact Factor 2014: 2.781, ISI Thomson Reuters Indexed)
2. **Amgad Ahmed Ali Ibrahim**, Abdul Manaf Hashim, “Statistical modelling and optimization of the growth of ultra-thin zinc oxide nanorods on graphene using ultrasonic spray pyrolysis”, *Nanoscale Res Lett*, 2015. Accepted. (Impact Factor 2014: 2.781, ISI Thomson Reuters Indexed)
3. **Amgad Ahmed Ali Ibrahim**, Abdul Manaf Hashim, “Evolution of ZnO nanowires based bird of paradise flower meso-structure: synthesis and optoelectronic properties”, *Nanoscale Res Lett*, 2015. Accepted. (Impact Factor 2014: 2.781, ISI Thomson Reuters Indexed)
4. **Amgad Ahmed Ali Ibrahim**, Abdul Manaf Hashim, “Computational analysis of the optical and charge transport properties of ultrasonic spray pyrolysis grown zinc oxide/graphene hybrid structures”, *Nanoscale Res Lett*, 2015. Accepted. (Impact Factor 2014: 2.781, ISI Thomson Reuters Indexed)

Publications Related to other work

1. Freddawati Rashiddy Wong, **Amgad Ahmed Ali Ibrahim**, Kanji Yasui, Abdul Manaf Hashim, “Seed/Catalyst-Free Growth of Gallium-Based Compound Materials on Graphene on Insulator by Electrochemical Deposition at Room Temperature”, *Nanoscale Res Lett*, 2015. 10:223. (Impact Factor 2014: 2.781, ISI Thomson Reuters Indexed).

2. Mohamed Mahmoud Nasef, Amgad Ahmed Ali Ibrahim, Hamidani Saidi, Arshad Ahmad, “Modelling and optimization aspects of radiation induced grafting of 4-vinylpyridene onto partially fluorinated films”, *Rad Phys Chem*, 2015. 94:1. (Impact Factor 2014: 1.38, ISI Thomson Reuters Indexed).

International Conferences

Main research

1. **Amgad Ahmed Ali Ibrahim**, and Abdul Manaf Hashim, “act of Density Functional Theory as a Tool for Process Design and Pre-Characterization of ZnO Growth on Graphene”, *8th International conference on materials for advanced technology ICMAT*, 28 June -3 July 2015, Singapore.
2. **Amgad Ahmed Ali Ibrahim**, and Abdul Manaf Hashim, “Growth of Zinc Oxide Nanostructures on Graphene by Ultrasonic Assisted Spray Pyrolysis and Its Modelling”, *8th International conference on materials for advanced technology ICMAT*, 28 June -3 July 2015, Singapore.
3. **Amgad Ahmed Ali Ibrahim**, and Abdul Manaf Hashim, “Growth of Zinc Oxide Nanostructures on Graphene by Ultrasonic Assisted Spray Pyrolysis and Its Modelling”, *27th Regional Conference on Solid State Science and Technology RCSSST27*, 20-22 December 2013, Kota Kinabalu, Malaysia.